Functional & Integrative Genomics (2023) 23:64
https://doi.org/10.1007/s10142-023-00988-3

ORIGINAL ARTICLE

Qi-Long-Tian capsule alleviates pulmonary fibrosis development by modulating inflammatory response and gut microbiota

Qiang Zhang[1] · Ting Luo[2] · Dezheng Yuan[3] · Jing Liu[3] · Yi Fu[4] · Jiali Yuan[1]

Received: 9 January 2023 / Revised: 13 February 2023 / Accepted: 14 February 2023 / Published online: 22 February 2023

Abstract

Pulmonary fibrosis (PF) is a chronic, progressive, and fibrotic interstitial lung disease with a high mortality rate. Qi-Long-Tian (QLT) capsule is an herbal formula with great potential for antifibrotic effects, consisting of San Qi (Notoginseng Radix et Rhizoma), Di Long [*Pheretima aspergillum* (E. Perrier)], and Hong Jingtian (Rhodiolae Crenulatae Radix et Rhizoma), and has been used in clinical practice for many years. To explore the relationship between the effects of Qi-Long-Tian capsule and gut microbiota of PF mice, pulmonary fibrosis model were established by tracheal drip injection of bleomycin. Thirty-six mice were randomly divided into 6 groups: control group (control), model group (model), QLT capsule low dose group (QL), QLT capsule medium dose group (QM), QLT capsule high dose group (QH), and pirfenidone group (PFD). After 21 days of treatment, after pulmonary function tests, the lung tissues, serums, and enterobacterial samples were collected for further analysis. HE staining and Masson's staining were used to detect changes as the main indicators of PF in each group, and the expression of hydroxyproline (HYP) related to collagen metabolism was detected by and alkaline hydrolysis method. qRT-PCR and ELISA were used to detect the mRNA and protein expressions of pro-inflammatory factors include interleukin 1β (IL-1β), interleukin 6 (IL-6), transforming growth factor β1 (TGF-β1), tumor necrosis factor α (TNF-α) in lung tissues and serums, and the inflammation-mediating factors include tight junction protein (ZO-1, Claudin, Occludin). ELISA was used to detect the protein expressions of secretory immunoglobulin A (sIgA), short-chain fatty acids (SCFAs), and lipopolysaccharide (LPS) in colonic tissues. 16sRNA gene sequencing was used to detect changes in the abundance and diversity of intestinal flora in the control, model, and QM groups, to search for differential genera, and analyze the correlation with inflammatory factors. QLT capsule effectively improved the status of pulmonary fibrosis and reduced HYP. In addition, QLT capsule significantly reduced the abnormal levels of pro-inflammatory factors, including IL-1β, IL-6, TNF-α, and TGF-β in lung tissue and serum, while improving the levels of pro-inflammatory related factors ZO-1, Claudin, Occludin, sIgA, SCFAs, and reducing LPS in the colon. The comparison between the alpha diversity and beta diversity in enterobacteria suggested that the composition of the gut flora in the control, model, and QLT capsule groups were different. QLT capsule significantly increased the relative abundance of *Bacteroidia* (which might limit the onset of inflammation) and decreased the relative abundance of *Clostridia* (which might promote inflammation). In addition, these two enterobacteria were closely associated with pro-inflammatory-related indicators and pro-inflammatory factors in PF. All these results suggest that QLT capsule intervenes in pulmonary fibrosis by regulating the differential genera of intestinal flora, increasing immunoglobulin secretion, repairing the intestinal mucosal barrier, reducing LPS entry into the blood, and decreasing inflammatory factor secretion in the serum, which in turn alleviates pulmonary inflammation. This study clarifies the therapeutic mechanism of QLT capsule in PF and provides a theoretical basis for it. It provides a theoretical basis for its further clinical application.

Keywords Qi-Long-Tian capsule · Pulmonary fibrosis · Inflammation · Pro-inflammatory factors · Intestinal flora

Qiang Zhang and Ting Luo contributed equally.

✉ Qiang Zhang
qiangzhang200000@163.com

✉ Jiali Yuan
jialiyuan650500@163.com

Extended author information available on the last page of the article

Abbreviations

cAMP	Cyclic adenosine monophosphate
Cchord	Quasi-static lung compliance
Claudin	Tight junction protein
ELISA	Enzyme linked immunosorbent assay
FEV50/FVC	50 Ms first expiratory volume/forced vital capacity

FRC	Functional residual capacity
GM	Gut microflora
HIV-1	Human immunodeficiency virus 1
HPLC	High performance liquid chromatography
HYP	Hydroxyproline
IL-1β	Interleukin 1β
IL-6	Interleukin 6
LPS	Lipopolysaccharide
MAPK	Mitogen-activated protein kinase
MMEF	Mean mid-expiratory flow
Occludin	Tight junction protein
OTU	Ovarian tumor domain
PCoA	Principal coordinate analysis
PEF	Peak expiratory flow
PF	Pulmonary fibrosis
PFD	Pirfenidone
QLT capsule	Qi-Long-Tian capsule
qRT-PCR	Real-time fluorescence quantitative PCR
SCFAs	Short-chain fatty acids
sIgA	Secretory immunoglobulin A
TGF-β1	Transforming growth factor β1
TLC	Total lung capacity
TNF-α	Tumor necrosis factor α
ZO-1	Tight junction protein

Introduction

Pulmonary fibrosis (PF) is a chronic, progressive, and heterogeneous scar disease. The pathogenesis of PF includes the theories of imbalance of inflammatory response, extracellular matrix deposition, epithelial mesenchymal transformation, and oxidative stress. Proliferation of interstitial fibroblasts and fibrotic changes of interstitial tissue are characteristics of PF (Guzy et al. 2017; Yu et al. 2021). Qi-Long-Tian (QLT) capsule is a traditional Chinese medicine prescription consisting of San Qi (Notoginseng Radix et Rhizoma), Di Long [*Pheretima aspergillum* (E. Perrier)], and Hong Jingtian (Rhodiolae Crenulatae Radix et Rhizoma). San Qi is recorded in the *Compendium of Materia Medica* as having the effect of stopping bleeding, dispersing blood, and fixing pain, as well as being widely cultivated in Yunnan Province. Di Long is one of the 67 animal medicines in the ancient Chinese medical book "*Shen Nong Ben Cao Jing*," which has the effects of clearing heat and relieving fright, promoting circulation, and calming asthma and diuretic. Hong Jingtian is an ethnic Yunnan medicine that grows in a highland environment and is commonly used in Tibetan medicine to treat chest pain and shortness of breath. QLT capsule was developed by Professor Fu Yi, a Qihuang scholar, and has obtained the production batch number: Dian (Z) 2020003A. QLT capsule is used as an in-hospital preparation in Kunming Chinese Medicine Hospital for the treatment of patients with pulmonary fibrosis. The summary of herbs in QLT capsule is shown in Fig. 1 (Wu et al. 2019). The main components of the herbs in QLT capsule are collected from the Traditional Chinese Medicine Systematic Pharmacology Database SymMap, TCMSP, and TCMID; in addition, we refer to the Chinese national knowledge infrastructure and PubMed to obtain compounds' information, which can be seen in Table 1 (Chen 2011; Ishaque, et al. 2012; Jówko et al. 2018; Panossian et al. 2010; Ru et al. 2014; Walker and Robergs 2006; Wu et al. 2019; Zhao et al. 2021a, b).

Gut microflora (GM) is a huge and complex microecological environment that has evolved to form a mutually beneficial symbiotic relationship with the host. The gut provides a suitable living environment for microbial growth and reproduction, while the gut microflora plays an important role in maintaining the homeostasis of the gut environment, nutrient metabolism, and health (Zhou et al. 2021). The gut is co-populated with probiotics, commensal bacteria, and potential pathogens that interact with the body's metabolic and immune systems to maintain the health of the host. However, factors such as unhealthy lifestyle, antibiotic abuse, mental stress, and food consumption could influence the balance of transgenic components and lead to the onset and development of diseases (Li et al. 2022). It has been reported (Chunxi et al. 2020) that dysbiosis of the gut bacteria not only interferes with the immune response of the intestine but also affects the immunity of distal organs including the pulmonary, further affecting the lung health and leading to respiratory diseases. Meanwhile, an experimental study (Gong et al. 2021) found a correlation between pulmonary fibrosis and GM, which are associated with PF indicators, as typified by 412 microbial community genera, 26 metabolites with the same trend of alteration, as well as 7 microorganisms and 9 metabolites. The above reports suggest a strategy to treat PF by modulating GM.

Recently, accumulating evidence suggests that herbal medicines, including compounds, extracts, and formulations, significantly modulate intestinal bacterial composition to intervene in disease development (Huang et al. 2017; Xia et al. 2020a, b; Xia et al. 2020a, b). Oral administration of QLT capsule, which requires digestion through the gastrointestinal tract and thus exerts its effect in alleviating pulmonary fibrosis, in which the GM might play an important role. Previous studies have shown that QLT capsule improves respiratory resistance to infection by reducing inflammatory and fibrogenic factors (Pi 2020; Leng et al. 2016; Fu et al. 2021; Zhang et al. 2022). Thus, we hypothesized that QLT capsule have a role in mitigating the development of pulmonary fibrosis by modulating the composition of GM. To verify this hypothesis, we did studies via building models, assessing drug effectiveness, detecting pro-inflammatory factors, and analyzing intestinal flora to clarify the therapeutic mechanism by which QLT capsule regulates GM, reduces inflammatory response, and achieves intervention in PF.

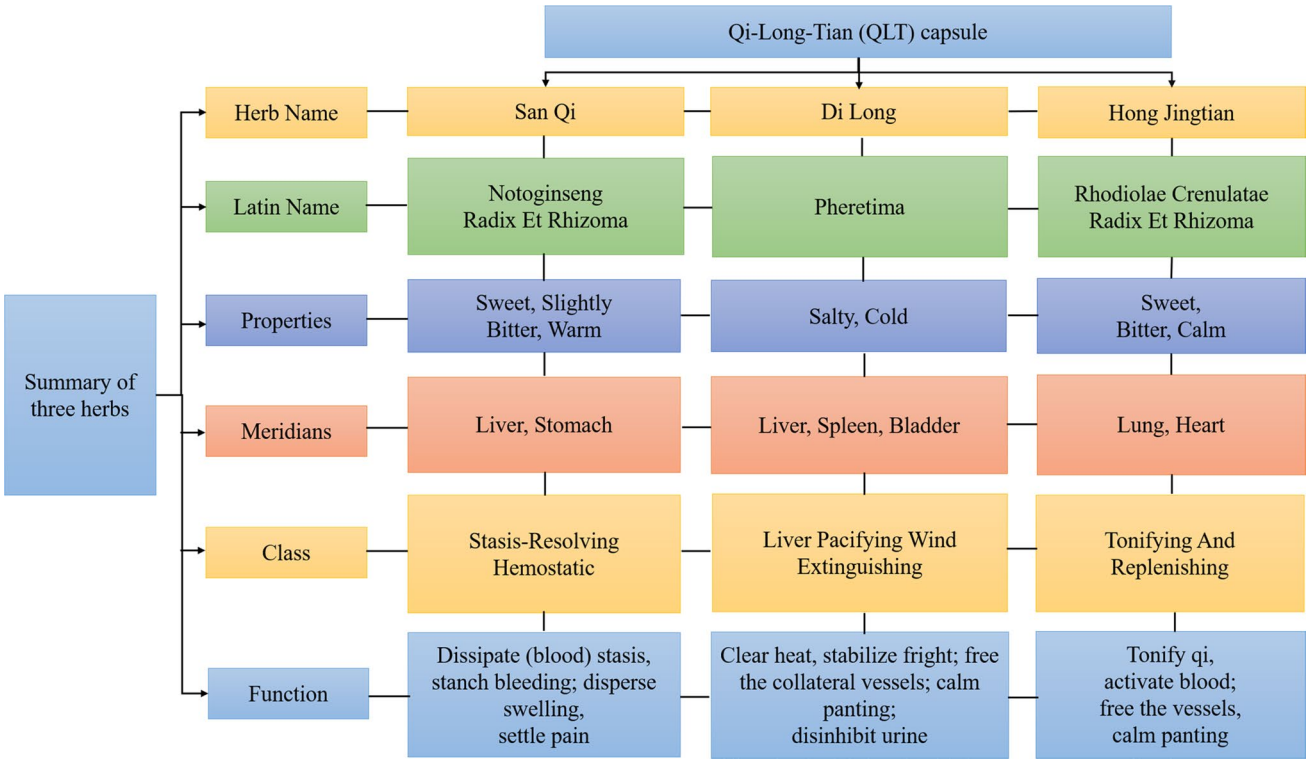

Fig. 1 The summary of herbs in QLT capsule

Materials and methods

Preparation of drugs

QLT capsule [No. Dian (Z) 2020003A] was prepared by Kunming Traditional Chinese Medicine Hospital (Yunnan, China) according to the standard production process. The proportion of the formula was San Qi (Notoginseng Radix et Rhizoma, #200601, 6 g), Di Long (*Pheretima*, #210101, 15 g), Hong Jingtian (Rhodiolae Crenulatae Radix et Rhizoma, #200801, 30 g). The herbs were immersed in water overnight and decocted twice (2 h for the first decoction and 1 h for the second). The tonics were combined and freeze-dried to obtain the powder (0.4 g per capsule, equivalent to 1.53 g of decoction pieces). The recorded peaks were determined by HPLC fingerprint analysis method (see Supplementary 1) to be used for quality control of QLT capsule. In vivo studies, the powder was reconstituted with the indicated concentrations of physiological saline. The positive drug was selected as pirfenidone (PFD, approval number: H20133376, Beijing Contini Pharmaceutical Co., Ltd., Beijing, China). Pirfenidone is a drug for IPF with good anti-inflammatory properties.

Animal experiments

Thirty-six male (Furman et al. 2022; Totsch et al. 2018; Tucker et al. 2017) C57BL/6 J mice, SPF, 4 weeks, 20 ± 2 g, were purchased from (Chengdu Dashuo Experimental Animal Co., Ltd., Sichuan, China [batch number: SCXK (Sichuan) 2020–030]. According to the guidelines for the care and use of experimental animals published by the National Institutes of Health and the guidelines of the Animal Ethics Experimental Committee of Yunnan University of Chinese Medicine, the experiments were approved for implementation [Yunnan University of Traditional Chinese Medicine Animal Experiment Ethics Committee, animal experimentation license number: SYXK (Dian) No.: K2022-0004]. Laboratory conditions were at controlled temperature (22 ± 3 °C), 12 h light and dark cycle, with free diet and water ingestion (animal ethics license number: R-06202023).

The mice were randomly divided into control dose group (control), model dose group (model), PFD dose group (PFD), QLT capsule low dose group (QL), QLT capsule medium dose group (QM), and QLT capsule high dose group (QH) by random number table method, 6 mice in each group. Adapted feeding for 1 week, the mice were modeled by single injection of bleomycin (approval

Table 1 The main compounds in herbs of QLT capsule

ID	Compound	OB (%)	ID	Compound	OB (%)
MOL000066	Alloaromadedrene	53.4614	MOL003958	Evodiamine	86.0162
MOL000069	Palmitic acid	19.2966	MOL003963	Hydroxyevodiamine	72.1074
MOL000175	Cyperene	51.1046	MOL004014	Evodiamine	73.77
MOL000346	Succinic acid	29.6203	MOL004017	Fordimine	55.1138
MOL000358	Beta-sitosterol	36.9139	MOL004018	Goshuyuamide I	83.1879
MOL000394	Choline	0.474665	MOL004020	Gossypetin	35.0026
MOL000415	Rutin	3.20153	MOL004021	Gravacridoneshlirine	63.7338
MOL000612	(−)-Alpha-cedrene	55.561	MOL004102	2-Coumarate	53.6043
MOL000635	Vanillin	51.996	MOL005319	Di-tert-butyl phthalate	43.6687
MOL000666	Hexanal	55.707	MOL005344	Ginsenoside Rh2	36.3195
MOL000675	Oleic acid	33.1284	MOL005369	Mycosinol	82.124
MOL000701	Quercitrin	4.03765	MOL005378	Panaxytriol	33.7583
MOL000842	Sucrose	7.17082	MOL005538	Linolenyl alcohol	42.8223
MOL000935	Hepanal	53.8332	MOL005729	1-Octen-3-Ol	15.2184
MOL001101	Alpha-ocimene	21.4314	MOL005749	Isopulegone	64.3102
MOL001304	2-Acetylpyrrole	58.3741	MOL005843	1-Hydroxycumene	59.9736
MOL001439	Arachidonic acid	45.5732	MOL006946	Adenosine	19.8532
MOL001456	Citric acid	56.2199	MOL006956	Cyclo-(Leu-Tyr)	111.16
MOL001464	Histamine	44.1042	MOL007088	Cryptotanshinone	52.342
MOL001494	Mandenol	41.9962	MOL007134	Danshensu	36.9148
MOL001604	Linalool	49.3674	MOL007349	Phosphatidylinositol	8.96258
MOL001739	Zoomaric acid	35.7759	MOL007460	Cyclooctadiene	43.3132
MOL001949	Panaxynol	42.7917	MOL007467	2,6-Dimethyl-cyclohexanol	76.2834
MOL002046	Hexanoic acid	73.0752	MOL007475	Ginsenoside F2	36.4317
MOL002379	Pentanal	59.5306	MOL007501	Panaxydol	61.6666
MOL002662	Rutaecarpine	40.3005	MOL007502	Nsc692928	43.5933
MOL002665	Ferulic acid	40.4343	MOL007508	A-Cyperene	51.1046
MOL002818	Piceol	36.8044	MOL007511	(5S)-5-Ethyloxolan-2-one	75.6885
MOL002850	Butylated hydroxytoluene	40.0203	MOL008890	Diethylamine	61.4356
MOL002929	Salidroside	7.01026	MOL008994	Alpha-cuparenol	55.7006
MOL002930	Tyrosol	33.8119	MOL009653	Cycloeucalenol	39.7265
MOL003050	Nonanoic acid	40.5089	MOL009842	Cytochrome C	5.45165
MOL003942	Rutaevine	66.0526	MOL010856	Putrescine	81.2251
MOL003943	Ranitidine	40.8903	MOL011443	Trilinolein	34.9108
MOL003956	Dihydro rutaecarpine	42.4385	MOL012851	Notoginsenoside R1	4.27056

number: H20055883, Hanhui Pharmaceutical Co., Ltd.) (5 mg/kg) by endotracheal intubation. The modeling operation is as follows. After weighing the mice in each group, the mice were anesthetized with 1% sodium pentobarbital solution at 2 mg/kg, injected intraperitoneally, and the mice were fixed at an angle of 30° after stable breathing (Jia and Guo 2012; Laferriere and Pang 2020). The mice were fixed at 30° after respiratory stabilization. The exposed skin of the mice was gently lifted with small forceps, and 0.5 cm was cut longitudinally to slowly and bluntly separate the muscle so as to expose the trachea. A total of 0.05 ml of 0.9% NaCl solution was injected into the trachea of the control group, and 0.05 ml of bleomycin solution was injected into the trachea of the remaining mice in each group. After pulling out the needle, immediately put the mouse plate upright, left, and right hanging, about 30 s after being 30° sutured to the neck skin. The mice were gently put into the mouse cage and placed in an inclined position, and the modeling was completed.

The intervention with QLT capsule was started on the 14th day (Chen 2018) after modeling, while the positive drug group was intervened with PFD. Dosage and administration method: the drug conversion ratio is human to mouse = 1:0.0026 (Huang et al. 2004); each mouse is gavaged according to the standard of 0.1 ml per 10 g body mass; the control group and model group are gavaged with normal saline; the QL, QM, and QH groups were gavaged with 0.39 g/kg, 0.78 g/kg, and 1.56 g/kg, respectively; and

the pirfenidone group was gavaged with 0.78 g/kg. The drug was administered at 14 days after modeling, and the materials were taken 21 days after administration.

After the end of administration, the mice were fasted without water for 12 h and anesthetized with pentobarbital. At the end of administration, mice were fasted without water for 12 h. After pentobarbital anesthesia, invasive pulmonary function test was detected; blood was collected from the heart. The serum was separated by centrifugation for 15 min with 3000 r/min at 4 °C. The upper lobe of the right lung was taken for HE staining. The remaining lungs, serums, colons, and gut bacterium were placed at −80 °C for subsequent studies. The schematic diagram of the animal study design is shown in Fig. 2.

Invasive pulmonary function test

After administration, the mice were anesthetized with 1% sodium pentobarbital solution at 2 mg/kg (Laferriere and Pang 2020). After fixation, skin preparation, and disinfection, the exposed trachea was gently and passively separated. The trachea was cut horizontally between the tracheal cartilage rings. The trachea was lifted after threading, the intubation needle was inserted, and the pulmonary function instrument (model: crfm100, EMMS, UK) was connected; the related indexes of pulmonary function were recorded.

HE staining

Paraffin sections were used for dewaxing, hematoxylin staining, eosin staining, and dehydration sealing. After the above operations, the sections were dried, sealed with neutral gum, observed under the microscope, photographed, collected images, and analyzed.

Masson's staining

Paraffin sections were dewaxed to water, stained with potassium dichromate, iron hematoxylin, Ponceau red, acid fuchsin, phosphoric acid, aniline blue, differentiated, transparent sealed with neutral gum, observed under the microscope, photographed, collected images, and analyzed the results.

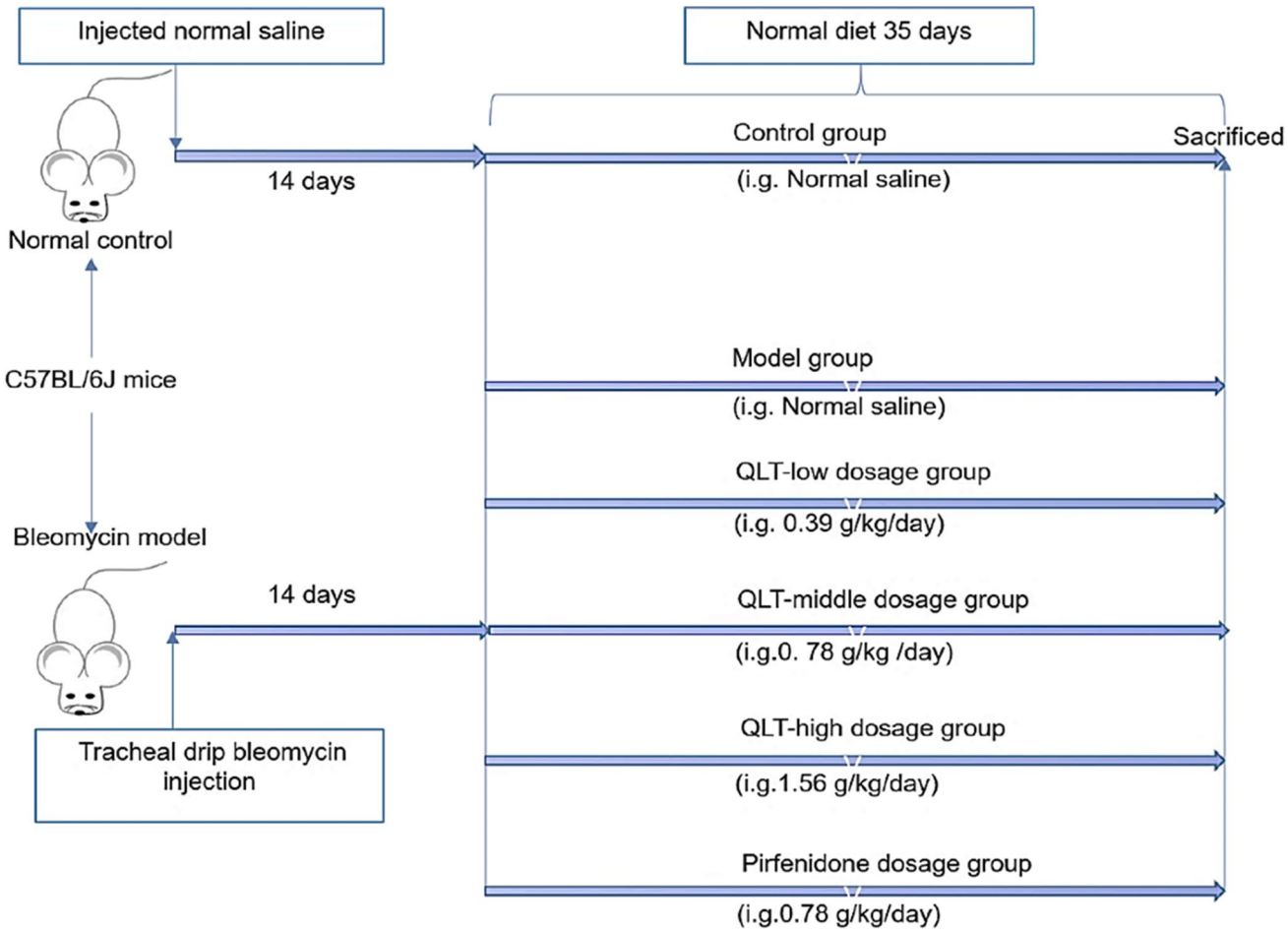

Fig. 2 The schematic diagram of the animal study design. Bleomycin model mice were used to assess the antidiabetic effect of QLT capsule

Hydroxyproline (HYP) detection

The HYP assay was measured with hydroxyproline determination kit (Cat#: A030-2–1, Nanjing Jiancheng Bioengineering Institute), following the product instruction book. Briefly, accurately weighted 30 mg mouse lung tissue and put into 1.5 ml tube. Hydrolysate 100 µl was added and gently blow and mixed. Tissue was hydrolyzed in boiling water for 20 min and mixed well every 10 min to insure sufficiently hydrolyzed. Then, add indicator 100 µl to each pipe after cooling with running water. Added 100% nail liquid into each tube, mixed and the solution turned red at this time; use 200 µl pipettes to add liquid B to the test tube drop by drop. After each drop is added, it needs to be mixed evenly until the solution turns yellow green (i.e., the red disappears). At this time, the pH value is about 6.0–6.8; add double distilled water to 1 ml, gently blow and mix. Absorb 300 µl dilute the hydrolysate, add about 25 mg activated carbon, mix well, centrifuge for 10 min at 4 °C, 3500 rpm, and absorb 100% after centrifugation supernatant, standby. After processing on the machine, take the 96-well plate and add 50 µl to each well after typesetting sample and add the configured standard solution 50 µl. The absorbance of each tube was measured with a microplate reader (BioTek Synergy H1, Agilent Technologies, Inc., USA) at a wavelength of 550 nm. HYP content (µg/ml) = (OD sample − OD control)/(OD standard − OD control) × standard concentration × (total volume of hydrolysate/wet weight of tissue).

Real-time fluorescence quantitative PCR (qRT-PCR)

The total tissue mRNA was extracted with Invitrogen™ TRIzol™ Reagent (Thermo Fisher Scientific Inc.). The primer sequences are listed in Table 1 and are synthesized by Sangon Biotech (Shanghai) Co., Ltd. The qPCR assay was measured by using Applied Biosystems QuantStudio 5 Real-Time PCR System (Thermo Fisher Scientific Inc.). The relative mRNA levels of each gene were calculated by using the $2-^{\Delta\Delta Ct}$ method (Table 2).

Enzyme linked immunosorbent assay (ELISA)

Samples were tested according to the ELISA kit instructions. The kits were mouse IL-1β ELISA kit (PI301, Beyotime), mouse IL-6 ELISA kit (PI326, Beyotime), mouse TGF-β1 ELISA kit (PT512, Beyotime), mouse TNF-α ELISA kit (PT878, Beyotime), mouse LPS ELISA kit (ab269542, Abcam), mouse Claudin ELISA kit (EKU11714, AmyJet Scientific), mouse Occludin ELISA kit (JL20408. Shanghai Jianglai industrial Limited by Share Ltd.), mouse ZO-1 ELISA kit (JL20409, Shanghai Jianglai industrial Limited by Share Ltd.), mouse sIgA ELISA kit (BS-2055, Bensheng (Tianjin) Health Technology Co., Ltd.), and mouse SCFAs ELISA kit (BS-9306, Bensheng (Tianjin) Health Technology Co.). The absorbance was measured, and the concentration was calculated using an enzyme marker (Synergy, BioTek, USA) at 550 nm. The absorptance was detected and concentrations were calculated using an enzyme marker (Synergy, BioTek, USA) at 550 nm.

16sRNA sequencing

The fecal samples were detected by Metabo-Profile Biotechnology (Shanghai) Co., Ltd. The samples were air-dried in a fume hood, and 100 mg of feces were extracted from the total DNA using the EZNA Tool DNA extraction kit (Omega, D4015). A total of 515F (GTGYCAGCMGCC GCGGT AA) and 806R (GGACTACNVGGGTWTCTAAT) were used to amplify the V3-V4 variable region of the 16S rRNA gene. Amplicons were purified using the QIAquick

Table 2 Sequences of qPCR primers

Gene names	Primer sequences
TGF-β1	Forward primer: 5′-AGCAACAATTCCTGGCGATACCTC-3′ Reverse primer: 5′-TCAACCACTGCCGCACAACTC-3′
TNF-α	Forward primer: 5′-CAGGCGGTGCCTATGTCTC-3′ Reverse primer: 5′-CGATCACCCCGAAGTTCAGTAG-3′
IL-6	Forward primer: 5′-CTTCCATCCAGTTGCCTTCTTG-3′ Reverse primer: 5′-AATTAAGCCTCCGACTTGTGAAG-3′
IL-1β	Forward primer: 5′-CAGGCAGGCAGTATCACTCA-3′ Reverse primer: 5′-AGCTCATATGGGTCCGACAT-3′
ZO-1	Forward primer: 5′-AGGACACCAAAGCATGTGAG-3′ Reverse primer: 5′-GGCATTCCTGCTGGTTACA-3′
Claudin	Forward primer: 5′-GAGACTACCACTGTCCCC-3′ Reverse primer: 5′-AAAGAATCCTCAAAACCA-3′
Occludin	Forward primer: 5′-ATAGCCATTGTCCTGGGGTTCAT-3′ Reverse primer: 5′-TCCATCTTTCTTCGGGTTTTCAC-3′
β-actin	Forward primer: 5′-GTCGTACCACAGGCATTGTGATGG-3′ Reverse primer: 5′-GCAATGCCTGGGTACATGGTGG-3′

PCR purification kit (QIAGEN, Germany). Library quality was assessed using a Qubit 2.0 fluorometer and Agilent Bioanalyzer 2100 system, and sequencing libraries were generated using NEBNEXT Ultra DNA. Libraries were sequenced on the Illumina Hiseq platform. Paired reads of 280 bp were generated after sequencing to analyze the composition of GM.

Statistical analysis

Experimental data were statistically processed by SPSS19.0 software and GraphPad prism 10.0 software. The measurement data were expressed by mean ± standard error of mean (SEM). When the sample accorded with normal distribution and the variance was homogeneous, the measurement data were analyzed by one-way ANOVA and intergroup comparison. The difference was statistically significant when $P < 0.05$.

Results

QLT capsule improved the pulmonary function of PF mice

As a necessary examination method for respiratory diseases, pulmonary function can be used as one of the diagnostic methods of PF. Quasi-static lung compliance (Cchord), mean mid-expiratory flow (MMEF), 50 ms first expiratory volume/forced vital capacity (FEV50/FVC), functional residual capacity (FRC), peak expiratory flow (PEF), and total lung capacity (TLC) reflect the pulmonary function severity of PF. The results show that compared with model group, QLT capsule significantly improved Cchord, MMEF, FEV50/FVC, FRC, PEF, and TLC value with dose-dependent, indicated that QLT capsule improved pulmonary function in PF mice (Fig. 3).

QLT capsule repairs the pulmonary tissue morphology of PF mice and reduces the hydroxyproline (HYP) content of lung tissue, which has the effect of alleviating the development of fibrosis

The HE staining showed that compared with control group, model group had inflammatory cell infiltration and alveolar space enlargement; compared with model group, PFD (pirfenidone), QLT capsule low (QL), QLT capsule medium (QM), and QLT capsule high (QH) dose groups could inhibit inflammatory cell infiltration and alveolar space enlargement (see Fig. 4a). Compared with control group, the HYP level was significantly higher in model group ($P < 0.01$); compared with model group, the HYP levels were significantly lower in PFD group, QL, QM, and QH groups ($P < 0.01$) (see Fig. 4b). The Masson staining showed that QLT capsule administration also reduced the area of pulmonary collagen deposition (Fig. 4c). The percentage of collagen deposition area in pulmonary tissues of the model group was significantly higher than that of the normal group ($P < 0.01$) and lower in the treatment of QLT capsule ($P < 0.05$) (see Fig. 4d).

QLT capsule decreased the mRNA and protein expressions of pro-inflammatory factors IL-1β, IL-6, TGF-β1, and TNF-α in the lung tissues of PF mice

The detection of mRNA and protein expressions on IL-1β, IL-6, TGF-β1, and TNF-α in the lung tissues for each group showed that compared with control group, the expressions of IL-1β, IL-6, TGF-β1, and TNF-α showed a significant increase in the model group (P 0.01); compared with model group, the expressions of IL-1β, IL-6, TGF-β1, and TNF-α were significantly decreased in each QLT capsule administration group ($P < 0.05$, $P < 0.01$) (see Fig. 5). The results indicated that QLT capsule effectively reduced the mRNA and protein expressions of pro-inflammatory factors in the lung tissues of mice with PF.

QLT capsule decreased the protein expressions of pro-inflammatory factors IL-1β, IL-6, TGF-β1, and TNF-α in the serums of PF mice

The detection of protein expressions on IL-1β, IL-6, TGF-β1, and TNF-α in the serums for each group showed that compared with control group, the expressions of IL-1β, IL-6, TGF-β1, and TNF-α showed a significant increase in the model group ($P < 0.01$); compared with model group, the expressions of IL-1β, IL-6, TGF-β1, and TNF-α were significantly decreased in each QLT capsule administration group ($P < 0.05$, $P < 0.01$) (see Fig. 6a–d). The results indicated that QLT capsule effectively reduced the protein expressions of pro-inflammatory factors in the serums of mice with PF.

QLT capsule increased the mRNA and protein expressions of tight junction proteins (ZO-1, Occludin, Claudin); the protein expressions of immunoglobulin A (sIgA), short-chain fatty acids (SCFAs), and decreased the protein expressions of lipopolysaccharide (LPS) in colonic tissues of PF mice

The detection on mRNA expressions of ZO-1, Occludin, and Claudin in colonic tissues showed that compared with control group, the mRNA expressions of ZO-1, Occludin, and Claudin were significantly decreased in the model

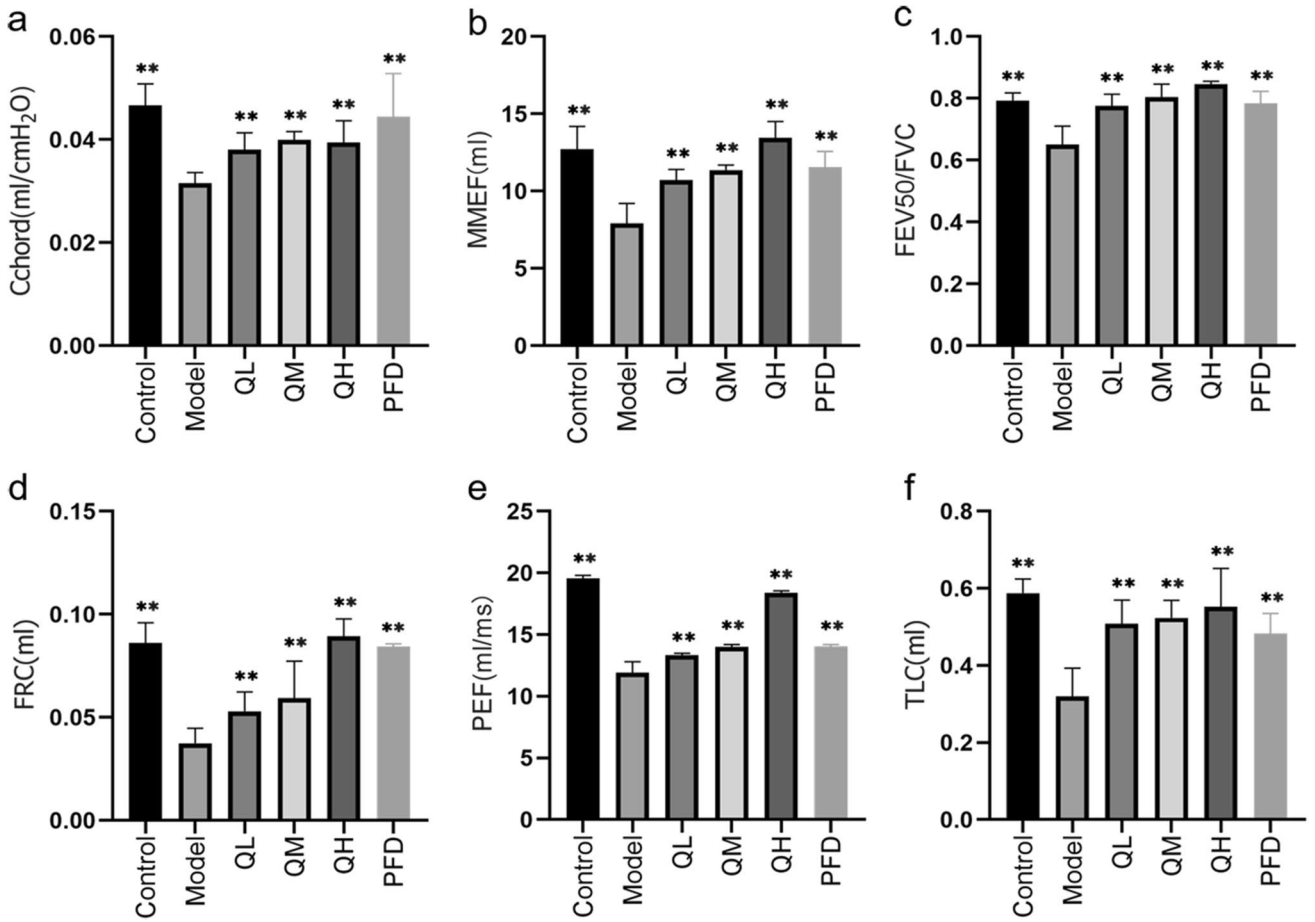

Fig. 3 Effects of pulmonary function in each group. **a** Cchord: an index reflecting lung compliance and expansibility, representing the effect of changes in thoracic pressure on lung volume. It reflects lung tissue elasticity and airway resistance. **b** MMEF: it reflects the detection index of pulmonary diffusion function. **c** FEV50/FVC: it is the volume of exhaled volume after maximum deep inhalation and maximum exhalation for 50 ms in mice. Obstructive or mixed type is slightly reduced to significantly reduced. **d** FRC: the decrease indicates PF. **e** PEF: it mainly reflects whether the large airway is blocked. **f** TLC: the decrease is mostly related to restrictive ventilation disorder, suggesting that it is related to PF. Data are expressed as mean ± SD. $^{**}P < 0.01$, compared with model group

group ($P < 0.01$); compared with model group, the mRNA expressions of ZO-1, Occludin, and Claudin were significantly increased in each QLT capsule administration group ($P < 0.01$) (see Fig. 7a–c). The detection on protein expressions of ZO-1, Occludin, Claudin, sIgA, and SCFAs in colonic tissues showed that compared with control group, the protein expressions of ZO-1, Occludin, Claudin, sIgA, and SCFAs were significantly decreased in the model group ($P < 0.01$); compared with model group, the protein expressions of ZO-1, Occludin, Claudin, sIgA, and SCFAs were significantly increased in each QLT capsule administration group ($P < 0.05$, $P < 0.01$) (see Fig. 7d–h). The detection on protein expression of LPS in colonic tissues showed that compared with control group, the protein expression of LPS was significantly decreased in the model group ($P < 0.01$); compared with model group, the protein expression of LPS was significantly increased in each QLT capsule administration group ($P < 0.05$, $P < 0.01$) (see Fig. 7i). The results indicated that QLT capsule could effectively increase the mRNA and protein expressions of tight junction proteins (ZO-1, Occludin, Claudin), the protein expressions of sIgA and SCFAs, as well as decrease the protein expression of LPS in colonic tissues with pulmonary fibrosis. The results might suggest that QLT capsule decreases pro-inflammatory-related factors in colonic tissues, which achieves the effect of alleviating PF inflammation.

The variation in the general composition of the groups was analyzed by specaccum accumulation and the Krona method

To explore the changes in QLT capsule enterobacterial microbes, we used 16S high-throughput sequencing to analyze the composition of enterobacterial microbes between control group, model group, and QLT capsule medium-dose group. QM (hereinafter referred to as QLT) was

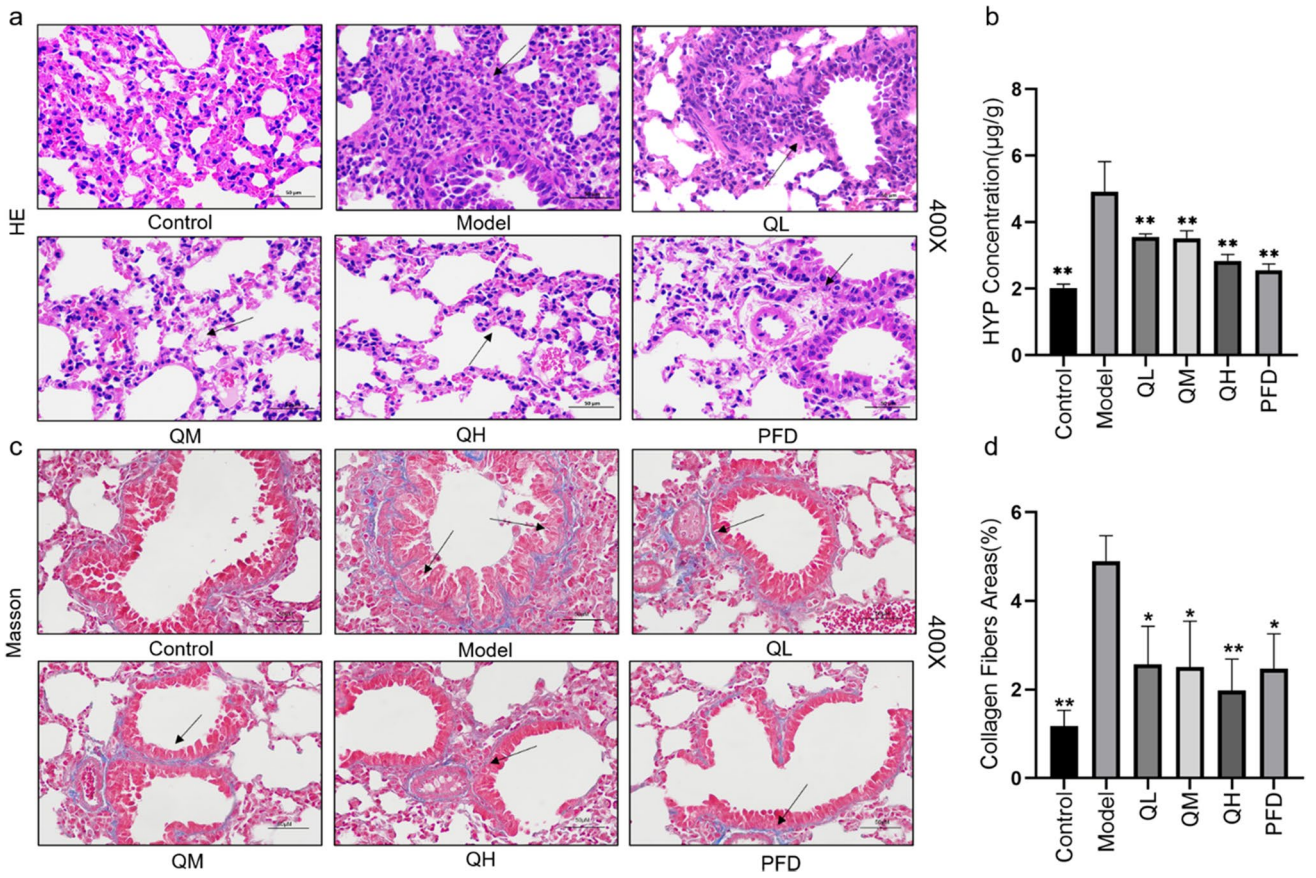

Fig. 4 QLT capsule alleviates fibrosis in PF mice. **a** HE staining (400×), **b** alkaline hydrolysis method for detection of HYP content, **c** Masson's staining (400×), **d** the percentage of collagen deposition area in pulmonary tissues. Arrows indicate pathological changes. Data are expressed as mean ± SD. $^{*}P < 0.05$, $^{**}P < 0.01$, compared with model group

chosen based on the aforementioned results showing that with treated PF mice, QLT capsule is dose-dependent, and that the medium-dose group is the clinically equivalent dose and more clinically directed. In this study, specaccum accumulation curves were used to describe the increase in species with increasing sampling size for samples from control group, model group, and QLT group, showing the adequacy of sample sampling size and the operability of predicting richness (Fig. 8a). The Krona analysis showed that the overall community composition of control group, model group, and QLT group was differential, indicating that diversity analysis of differential genera could be performed (Fig. 8b–d).

QLT capsule changed the GM composition in PF mice

The statistical results by Chao1, Observed, Simpson, and Shannon in α-diversity showed that compared with control group, the model group showed a decreasing trend; and compared with model group, the QM group showed an increasing trend, which indicated that QLT capsule increased the abundance of GM (see Fig. 9a–d). The results of principal coordinate analysis (PCoA) calculation by β-diversity showed that there was a visible clustering among the groups of control, model, and QM groups. Meanwhile, compared to model group, the QM and control groups are closer to each other in terms of dimensionality and perspective, which indicated that the clustering between QM and control groups is more close to each other (see Fig. 9e).

Changes of *Bacteroidia* and *Clostridia* in GM associated with inflammatory metabolic pathways and pro-inflammatory factors related to PF development

To further decipher the composition of GM changed by QLT capsule, we selected the genus level in GM for analysis. The results showed that after intervention by QLT capsule, the relative abundance of *Bacteroidia* among GM was significantly increased, and the relative abundance of *Clostridia*, *Acidobacteriia*, *Solibacteres*, *Coriobacteriia*,

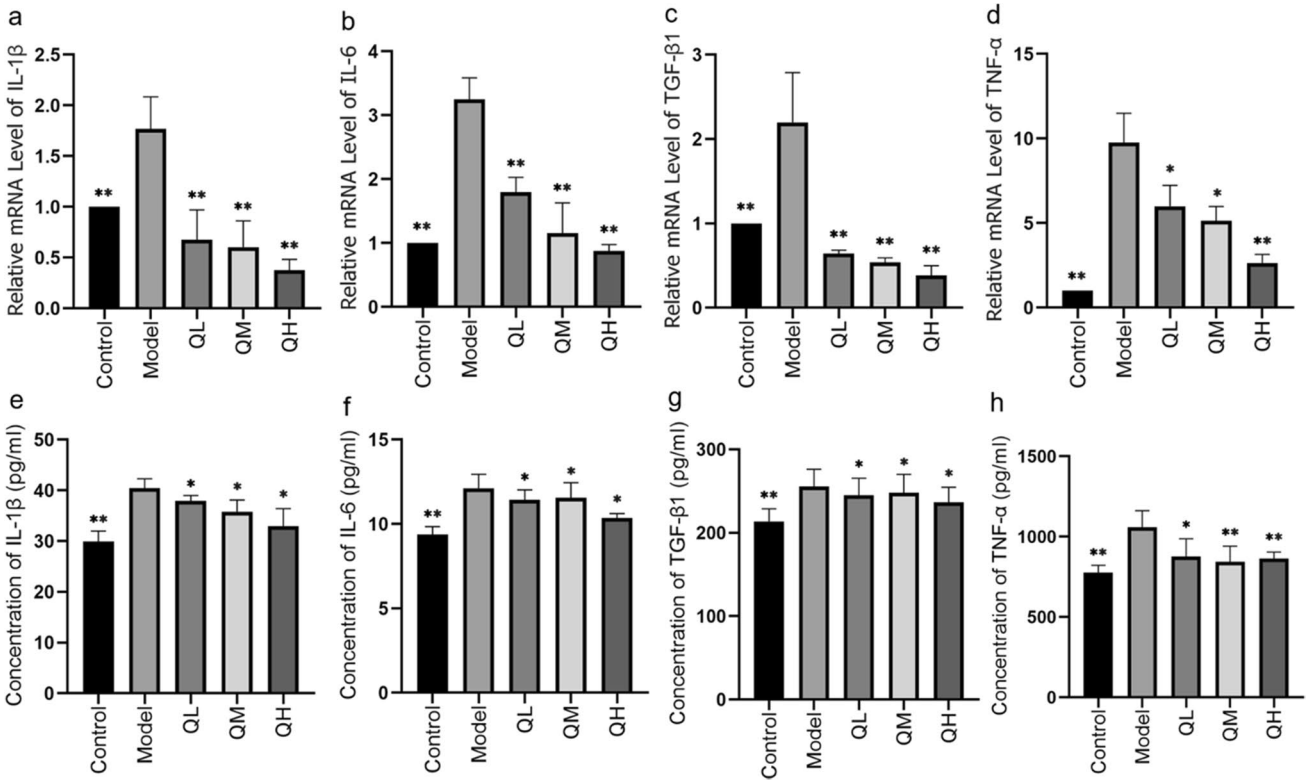

Fig. 5 QLT capsule decreased the mRNA and protein expressions of pro-inflammatory factors in the lung tissues of PF mice. qRT-PCR for mRNA expressions of **a** IL-1β, **b** IL-6, **c** TGF-β1, and **d** TNF-α in lung tissues. ELISA for protein expressions of **e** IL-1β, **f** IL-6, **g** TGF-β1, and **h** TNF-α in lung tissues. Data are expressed as mean ± SD. $^{*}P < 0.05$, $^{**}P < 0.01$, compared with model group

Cytophagia, *Flavobacteriia*, *Cyanobacteria*, chloroplast, and *Mollicutes* were downregulated. In addition, the relative abundance of *Clostridia* was significantly downregulated (see Fig. 10a). To further assess the interactions between QLT capsules, gut microbial composition and intestinal metabolic pathways, Picrust gene function prediction results were used. This was then compared with the Kyoto Encyclopedia of Genes and Genomes (KEGG) database to obtain the abundance of relevant pathways after intervention of QLT capsule. We analyzed the top 10 predicted pathways and found that QLT capsule increased the production of metabolic pathways associated with inflammatory diseases by GM including: *Staphylococcus aureus* infection, *Vibrio cholerae* infection, hypertrophic cardiomyopathy, renin-angiotensin system, Parkinson's disease; biometabolism-related pathways including: alpha-linolenic acid metabolism, D-arginine and D-ornithine metabolism xenobiotics biodegradation and metabolism; biosynthesis-related pathways including: biosynthesis of other secondary metabolites, flavone, and flavonol biosynthesis (see Fig. 10b). In addition, the relationships between PF pro-inflammatory factors, *Bacteroidia* and *Clostridia* in GM, were analyzed by Pearson's correlation analysis (see Fig. 10c). As shown in Fig. 9c, pro-inflammatory factors (IL-1β, IL-6, TGF-β1, TNF-α) in serums and pro-inflammatory-related factors (ZO-1, Occludin, Claudin, sIgA, SCFAs) in colonic tissues were negatively correlated with *Bacteroidia* and positively correlated with *Clostridia*; pro-inflammatory-related factor of LPS was positively correlated with *Bacteroidia* and negatively correlated with *Clostridia*. These results suggested that the changes in the composition of GM were closely related to the pro-inflammatory factors associated with the development of PF, and that *Bacteroidia* and *Clostridia* are more correlated with them.

Discussion

Qi-Long-Tian (QLT) capsule is a traditional Chinese medicine prescription consisting of San Qi (Notoginseng Radix et Rhizoma), Di Long [*Pheretima aspergillum* (E. Perrier)], and Hong Jingtian (Rhodiolae Crenulatae Radix et Rhizoma). San Qi is recorded in the *Compendium of Materia Medica* (Li et al. 2019) as having the effect of stopping bleeding, dispersing blood and fixing pain, as well as being widely cultivated in Yunnan Province. Di Long is one of the 67 animal medicines in the ancient Chinese medical book "*Shen Nong Ben Cao*

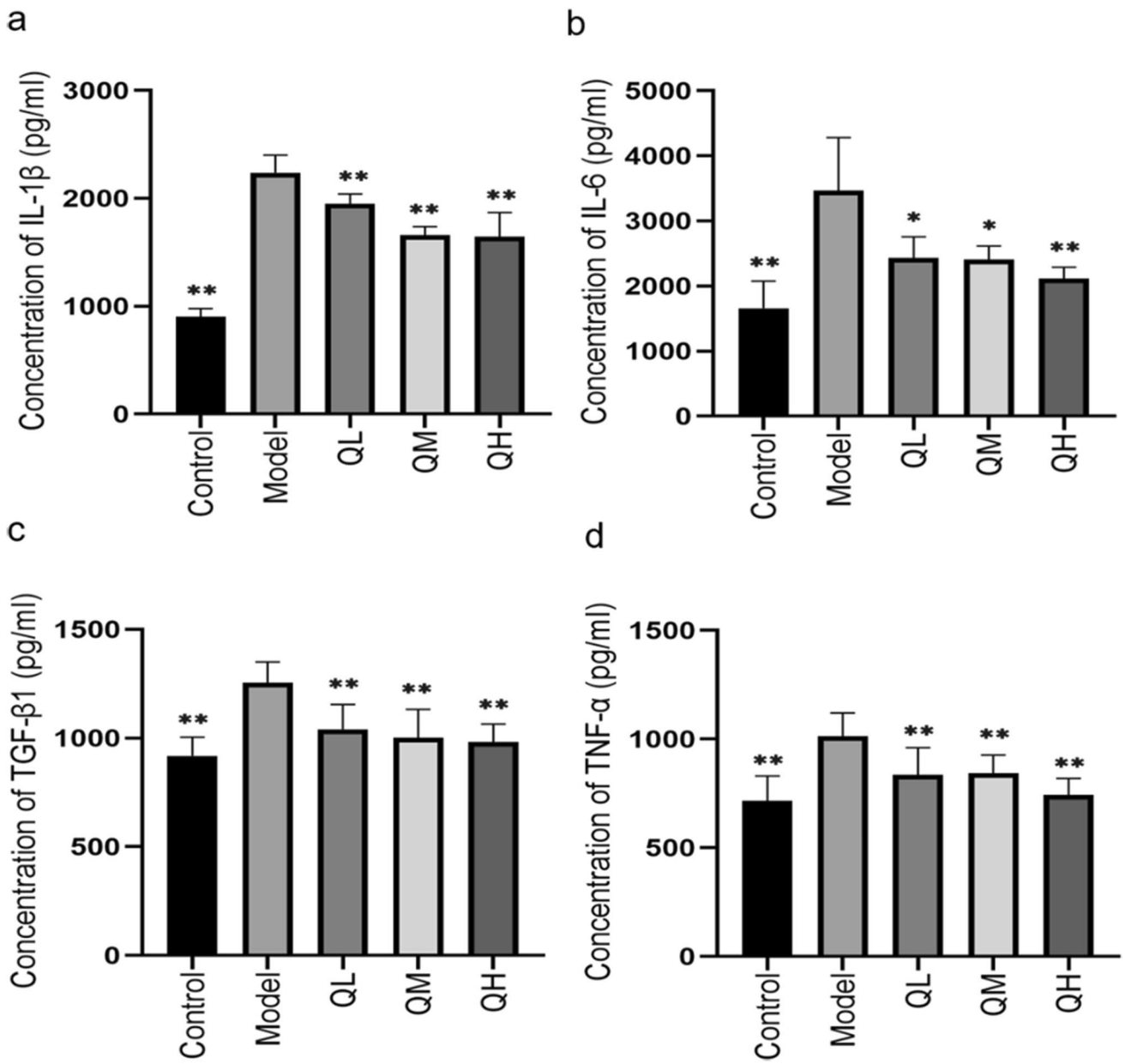

Fig. 6 QLT capsule decreased protein expressions of pro-inflammatory factors in serums of PF mice. ELISA for protein expressions of **a** IL-1β, **b** IL-6, **c** TGF-β1, and **d** TNF-α in serums. Data are expressed as mean ± SD. *$P < 0.05$, **$P < 0.01$, compared with model group

Jing" (Gu and Teng 2008), which has the effects of clearing heat and relieving fright, promoting circulation, and calming asthma and diuretic. Hong Jingtian is an ethnic Yunnan medicine that grows in a highland environment and is commonly used in Tibetan medicine to treat chest pain and shortness of breath (Pu et al. 2020). In recent years, QLT capsule has been used in Kunming Traditional Chinese Medicine Hospital as an in-hospital preparation [production lot number: Yunnan Pharmaceutical Production (Z) 2020003A] for the treatment of patients with pulmonary fibrosis. Pulmonary function examination is one of the necessary examinations for respiratory diseases and is mainly used to detect the patency of respiratory tract and the size of lung volume. It is of great value for detecting lung diseases, evaluating the severity and prognosis of diseases, and evaluating the efficacy of drugs or other treatment methods. The results show that compared with model group, QLT capsule significantly improved Cchord, MMEF, FEV50/FVC, FRC, PEF, and TLC value with dose-dependent, indicated that QLT capsule improved pulmonary function in PF mice ($P < 0.01$) (see Fig. 3), which is consistent with relevant research reports on pulmonary function (Milton et al. 2012). The accumulation of inflammatory cells and

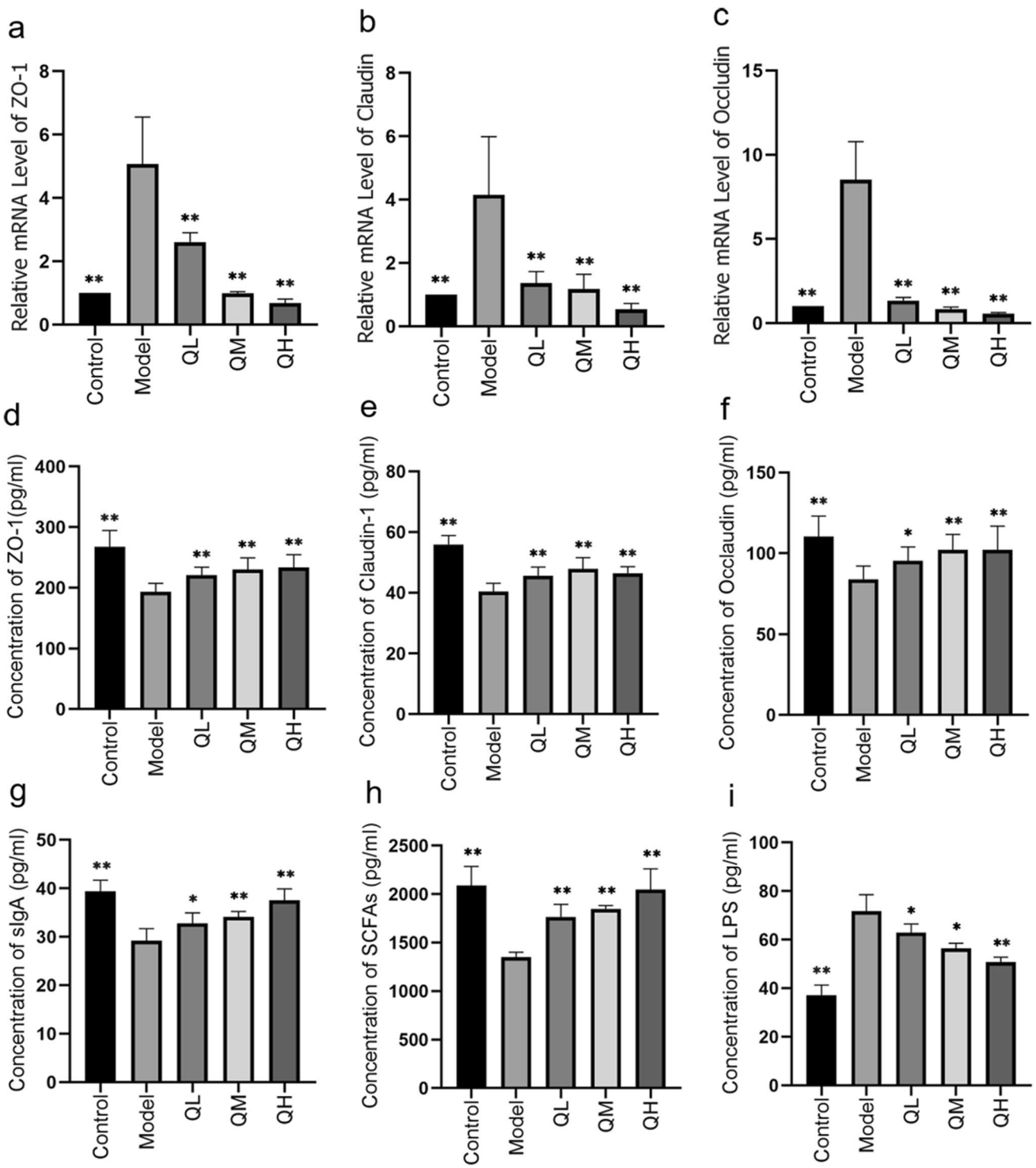

Fig. 7 QLT capsule decreased protein expressions of pro-inflammatory-related factors in colonic tissues. qRT-PCR for mRNA expressions of **a** ZO-1, **b** Occludin, and **c** Claudin in colonic tissues. ELISA for protein expressions of **d** ZO-1, **e** Occludin, **f** Claudin, **g** sIgA, **h** SCFAs, and **i** LPS in colonic tissues. Data are expressed as mean ± SD. $^{*}P < 0.05$, $^{**}P < 0.01$, compared with model group

the release of cytokines increase collagen fibers, leading to remodeling of lung tissue, reduction in the number of alveoli, deformation, atresia, and loss of lung function, which are the main pathological changes in PF (Nakerakanti and Trojanowska 2012). In order to clarify the pathology of PF and the restorative role of QLT capsule, this study was performed to

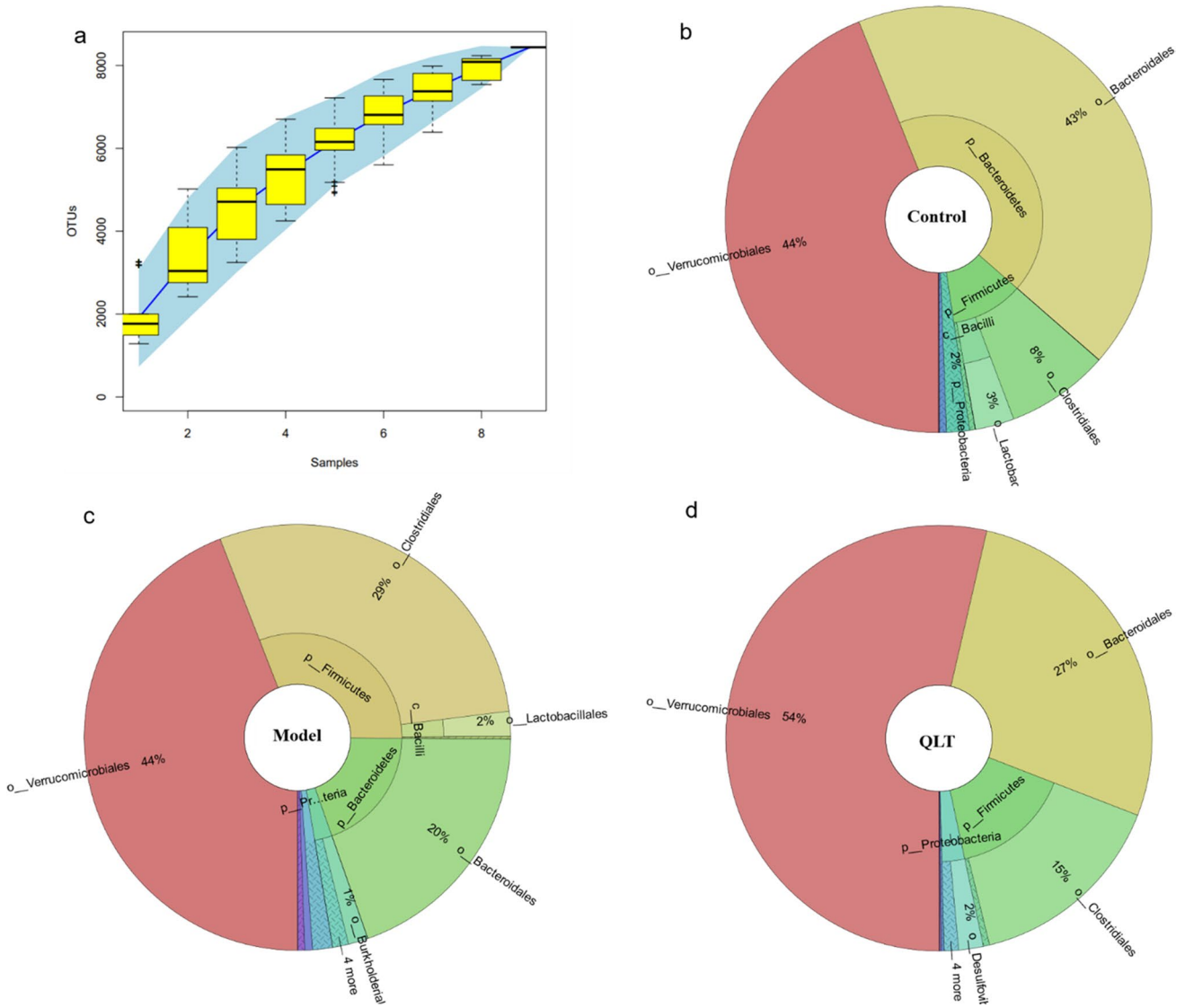

Fig. 8 Variation in the general composition of the groups. **a** Specaccum accumulation plots for all samples. *X*-axis represents the sample size, and *Y*-axis represents the number of OTUs detected, and the results reflect the rate of increase of new species observed as the sample size is continuously expanded over the course of sampling the overall sample. The Krona analysis is presented in the form of a circle diagram for **b** control group, **c** model group, and **d** QLT capsule group. The taxonomic levels of domains, phyla, orders, families, and genera are represented in order from inside to outside, and the size of the sectors reflects the relative abundance of different flora, which is distinguished by different colors for each flora

compare inflammatory cell infiltration and collagen deposition using HE and Masson's stainings. The results showed that morphology of lung tissue was observed by HE staining and the Masson staining. Compared with model group, QLT capsule significantly inhibited the infiltration of inflammatory cells and the expansion of alveolar space (see Fig. 4a). At the same time, QLT capsule inhibited the accumulation of collagen in the lung in a dose-dependent manner, in which the high dose is more effective (see Fig. 4b, c). Meanwhile, QLT capsule decreased the hydroxyproline (HYP) content in the pulmonary tissues of PF mice ($P < 0.01$) (see Fig. 4d), which indicated that QLT capsule had the effect of slowing down the development of fibrosis. The relationships between inflammation and pulmonary fibrosis are closely related.

Reports have shown that pulmonary inflammation is a common cause of PF, and the incidence of post-inflammatory pulmonary fibrosis is extremely high (Chopra et al. 2021; Ding et al. 2021; Liu et al. 2018; Lv et al. 2021; Meyer et al. 2021; Shaw et al. 2019; Zhan et al. 2020). Various pro-inflammatory factors can cause an inflammatory response, which in turn leads to the exacerbation of PF. Inflammatory cell break through the immune response and induce monocytes to transform into macrophages, which promote interstitial degradation by secreting inflammatory factors such as IL-1β,

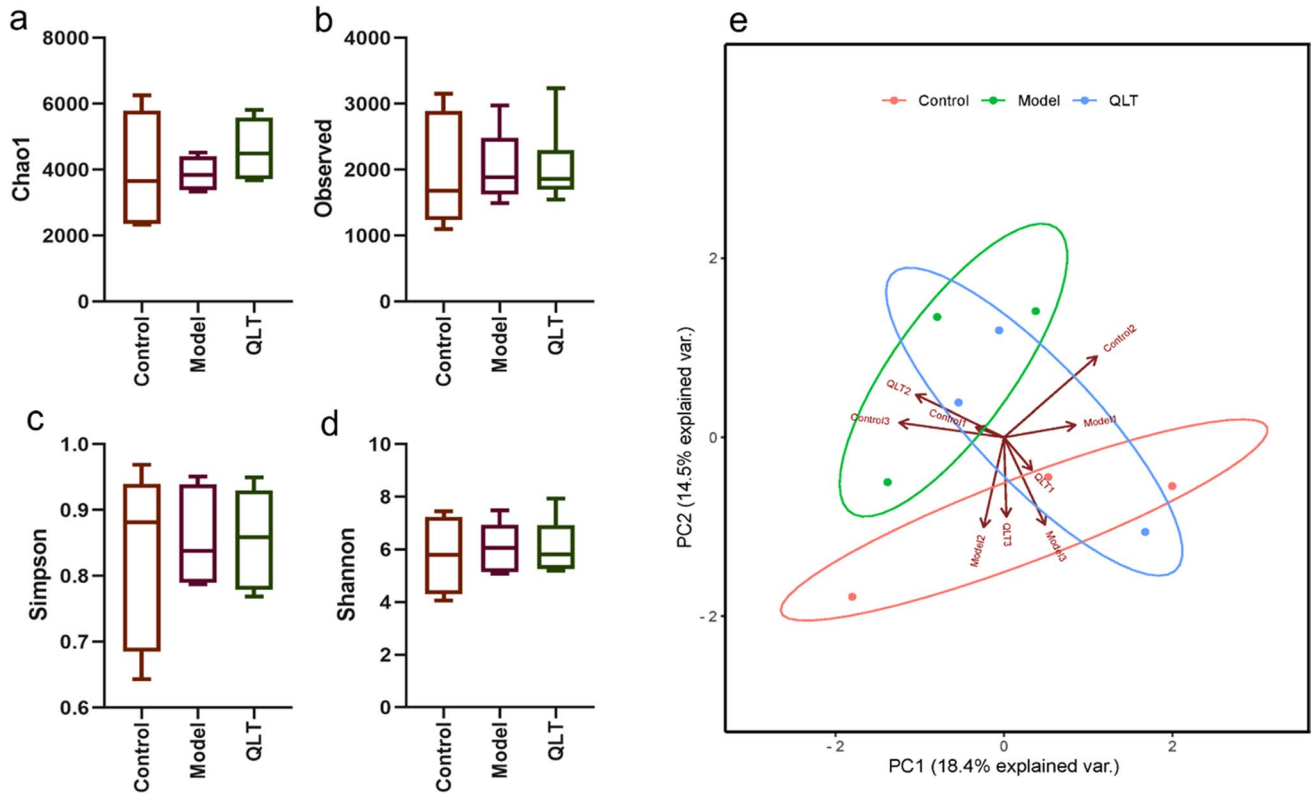

Fig. 9 QLT capsule changed the GM composition. α-Diversity for 16S sequencing data **a** Chao1, **b** Observed, **c** Simpson, and **d** Shannon. β-diversity for 16S sequencing data **e** PCoA results (*X*- and *Y*-axes are distances between samples, red circles represent control group, green circles represent model group, blue circles represent QM group)

IL-6, TGF-β1, and TNF-α with matrix metalloproteinases, leading to inflammatory cell infiltration, damaging the tissue surrounding, and exacerbating alveolar damage (Chen and Xu 2022; Dai et al. 2017; Khan et al. 2015; Venturin et al. 2016; Zhang et al. 2012). In this study, we indicated that compared with control group, the expressions of IL-1β, IL-6, TGF-β1, and TNF-α showed a significant increase in the model group ($P<0.01$); compared with model group, the expressions of IL-1β, IL-6, TGF-β1, and TNF-α were significantly decreased in each QLT capsule administration group ($P<0.05$, $P<0.01$) (see Fig. 5). The results suggested that QLT capsule effectively reduced the mRNA and protein expressions of pro-inflammatory factors in the lung tissues of mice with PF. Meanwhile, the protein expressions of IL-1β, IL-6, TGF-β1, and TNF-α in the serums of PF mice were significantly increased ($P<0.05$, $P<0.01$), while QLT capsule decreased the protein expressions of IL-1β, IL-6, TGF-β1, and TNF-α ($P<0.05$, $P<0.01$) (see Fig. 6). This indicates that QLT capsule effectively reduced the protein expressions of pro-inflammatory factors in the serums of PF.

Tight junctions are usually located between adjacent cells at the apical part of epithelial cells. The tight junction molecule is composed of peripheral cytoplasmic proteins such as occluding small band protein (ZO-1), tight junction proteins (Claudins), and Occludin. The three proteins are localized at the cell junctions and constitute important proteins for the function of the tight junction barrier, which play a key role in maintaining the integrity of the tight junctions and defense against pathogens (Hsu et al. 2017; Zhao et al. 2009). The intestinal mucosal barrier is the first barrier of the intestine against foreign invasion, and its core structure is tight junctions, which are widely present between adjacent intestinal epithelial cells (Martin and Jiang 2009). The results indicated that QLT capsule could effectively increase the mRNA and protein expressions of ZO-1, Occludin, and Claudin of colonic tissues in PF (see Fig. 7a–f). This suggested that the expression of tight junction protein in colonic tissues was reduced in the presence of PF, while QLT capsule increased the tight junction protein in colonic tissues and enhanced the resistance of the organism.

Since the first line for the organism to resist disease is the mucosa, secretory immunoglobulin A (sIgA) plays an important role as the main antibody of mucosal immunity. sIgA is mainly produced through activated B cells in the human mucosa. It is secreted into the exocrine fluid and becomes the main antibody for mucosal immunity (Jia et al. 2013). In this study, we have shown that compared with control group, the protein expression of sIgA showed a significant decrease in model group ($P<0.01$);

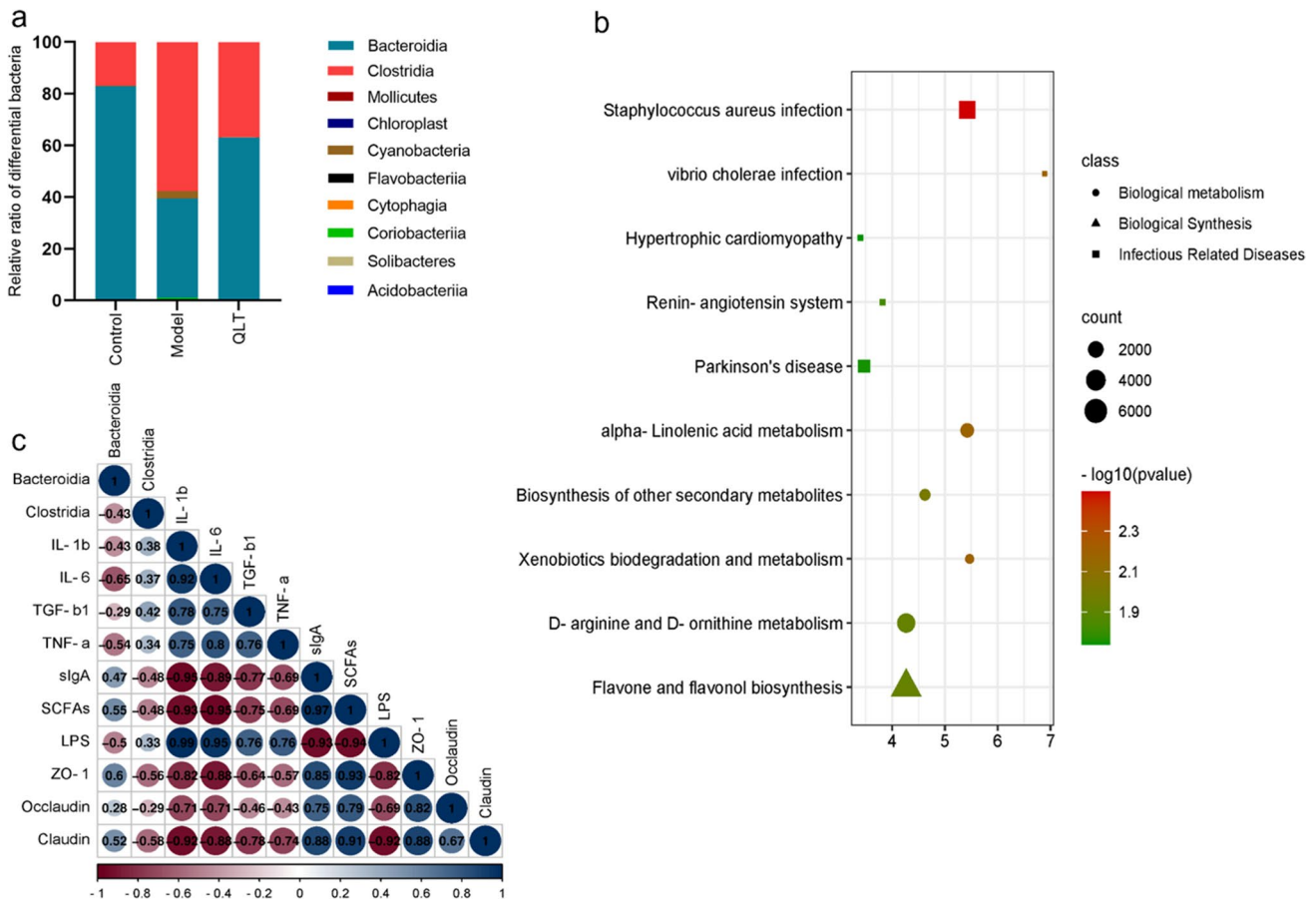

Fig. 10 Changes of *Bacteroidia* and *Clostridia* in GM associated with inflammatory metabolic pathways and pro-inflammatory factors related to PF development. **a** Stacked bar graph shows the ratio of each group with differential GM (top 10), *X*-axis represents the group and *Y*-axis represents the ratio. Each bar represents a group, and each color represents one microorganism at the genus level; the longer the bar, the higher the abundance of the corresponding species. **b** KEGG analysis of intestinal metabolic pathways (*X*-axis represents enrichment fold, *Y*-axis represents top 10 pathway names) (The size of the dots represents the number of target genes, and the color of the dots represents the range of FDR, which indicates the ratio of pathway target genes to the number of all annotated genes in the pathway). **c** Pearson's correlation analysis between *Bacteroidia*, *Clostridia*, and PF development pro-inflammatory factors (*X*-axis represents the values, *Y*-axis represents the indexes compared, the numbers in the circles are the calculation of correlation, −1 to 0 is negative correlation, 0 to 1 is positive correlation, the shade of the circle color represents the magnitude of the value).

compared with model group, the protein expression of sIgA in each QLT capsule administration group showed a significant increased ($P<0.05$, $P<0.01$) (see Fig. 7g). It was suggested that QLT capsule could effectively increase the protein expression of sIgA in colonic tissues with PF.

Short-chain fatty acids (SCFAs) are important metabolites of GM. In macrophages, neutrophils and dendritic cells, SCFAs can regulate the expression of genes related to inflammation and immunity by activating the mitogen-activated protein kinase (MAPK) pathway through G protein-coupled receptors, inhibiting the β-arrestin2/NF-κB pathway, suppressing the synthesis of cyclic adenosine monophosphate (cAMP), and promoting the entry of calcium ions (Ca^{2+}) into the nucleus (Yao et al. 2022). In this study, compared with control group, the protein expression of SCFAs was significantly decreased in model group ($P<0.01$); compared with model group, the protein expression of SCFAs was significantly increased in each QLT capsule administration group ($P<0.05$, $P<0.01$) (see Fig. 7h). It was suggested that QLT capsule could effectively increase the protein expression of LPS in the colonic tissues with PF.

Lipopolysaccharide (LPS) is a compound containing sugars and lipids. It is a major component of the outer membrane in gram-negative bacteria. When GM is imbalanced, a large number of gram-negative bacteria lyse LPS in death and release it into the intestine. When the intestinal mucosal barrier is damaged, LPS enters the circulatory system and activates multiple intracellular signal transduction pathways, causing a massive release of inflammatory factors and forming inflammatory responses, resulting in damage to the organism (Khan et al. 2017). In this study, compared with control group, the protein expression of LPS was significantly increased in model group

($P < 0.01$); compared with model group, the protein expression of LPS was significantly decreased in each QLT capsule administration group ($P < 0.05$, $P < 0.01$) (see Fig. 7i). It was suggested that QLT capsule could effectively reduce the protein expression of LPS in the colonic tissue with PF.

In recent years, the medical science has developed a "pulmonary-intestinal axis" and found that GM is crucial for lung diseases (Limeta et al. 2020). It is believed that the main roles of GM include biological barrier (Iacob and Iacob 2019), metabolic regulation (Wu et al. 2021), and immunomodulation (Guo 2021; Mercader-Barceló et al. 2020). Changes in GM lead to dysregulation of immune function, and studies have shown that GM regulate the differentiation of immune cells in the tissues associated with the intestinal mucosa and induce an inflammatory response in the body (Adan et al. 2019). Previous studies have shown that GM has an important regulatory role in the bidirectional pathway between the intestine and respiratory system, participating in the development of respiratory system functions and pathologies, and an increase or decrease in the type and number of GM might raises the chance of several diseases (Schneiderhan et al. 2016). Therefore, when the bidirectional regulatory homeostasis of the pulmonary-intestinal axis mediated by GM is disrupted, it induces respiratory diseases in the organism. As reported, a large reduction in the phylum *Firmicutes*, *Bacteroides* mimicus, may increase the chance of idiopathic pulmonary fibrosis in elderly patients (Guo 2021). α-Diversity is one of the important evaluation criteria in microecological studies, mainly through the magnitude of α-diversity index to measure the diversity, richness, evenness, coverage, etc. of microbial species in each group of community samples. The Chao1 and Observed species indices characterize the richness, and the Shannon and Simpson indices characterize the diversity. β-Diversity is often used to compare the differences between different colonies and reflects the heterogeneity between biological species. In layman's terms, it is a change in the distribution of species and is often calculated and analyzed by using PCoA (Liu et al. 2021; Choudhury et al. 2021). In this study, the variation in the general composition of the groups was analyzed by specaccum accumulation and the Krona method, which indicates that diversity analysis of differential genera could be performed (see Fig. 8). We indicated that the α-diversity of GM was reduced in pulmonary fibrosis mice and improved after administration of QLT capsule (see Fig. 9a–d). The results of β-diversity analysis showed that the differences in GM structure between control and model groups were greater, and the differences in GM structure between QLT capsule and control mice groups were lower (see Fig. 9e). Meanwhile, metabolic pathways could further clarify the correlation between enterobacteria and inflammation (Nie et al. 2021; Sato et al. 2021; Wu et al. 2022). By predicting the abundance of related pathways, among the top 10 pathways, there were five metabolic pathways that increased the production of inflammation-related diseases by enterobacteria after the intervention of QLT capsule: *Staphylococcus aureus* infection, *Vibrio cholerae* infection, hypertrophic cardiomyopathy, renin-angiotensin system, and Parkinson's disease (see Fig. 10a). This further suggests that QLT capsule is involved in intervening in the role of enterobacteria associated with inflammation. Our study further screened for 2 major differential genera, *Bacteroidia* and *Clostridia* (see Fig. 10b). It was reported that *Bacteroidia* could be increased in human immunodeficiency virus 1 (HIV-1) infected individuals, which limit chronic pathological immune activation in HIV-1 infection (Abdool Karim et al. 2019; Ling et al. 2016; Paquin-Proulx et al. 2017). In another study report, it was suggested that continuous depletion of *Bacteroidia* might increase oral-derived pathogens and exacerbate the development of colorectal cancer (Zhao et al. 2021a, b). In a report of inflammatory bowel disease, it was also shown that persistent intestinal inflammatory immune response leads to depletion of *Bacteroidia* (Stecher 2015). In a study reported on *Clostridia* and necrotizing small intestinal colitis, the presence of *Clostridia* colonization was considered extremely harmful (Schönherr-Hellec and Aires 2019). Pathogenic *Clostridia*, as an enteropathogenic bacterium (Guan and Goldfine 2021), might also induce pseudomembranous colitis (Roberts and Hughes 1985). In this study, pro-inflammatory factor indicators in serum (IL-1β, IL-6, TGF-β1, TNF-α) and pro-inflammatory-related factors in colonic tissue (ZO-1, Occludin, Claudin, sIgA, SCFAs) were negatively correlated with *Bacteroidia* and positively correlated with *Clostridia*; the pro-inflammatory-related factor LPS in colonic tissue was positively correlated with *Bacteroidia* and negatively correlated with *Clostridia*, which are consistent with the studies reported above (see Fig. 10c). The overall study concept is been shown in Fig. 11.

The limitations of this study include the absence of experiments with the addition of alveolar lavage fluid for the inflammatory response to pulmonary fibrosis. Pathological changes of inflammation were not evident in HE sections of colonic tissue. Due to limited funding, we were unable to perform western-blotting experiments for relevant inflammatory factors. In addition, the clearing experiments for GM are to be investigated in subsequent studies.

Conclusion

In this study, QLT capsule was shown to repair pulmonary tissue morphology and reduce collagen deposition and HYP content in PF mice, which has an effect on alleviating the development of fibrosis. QLT capsule decreased the expressions of pro-inflammatory factors (IL-1β, IL-6, TGF-β1, TNF-α) in the lung tissues and serums of PF. QLT capsule increased expressions of tight junction proteins (ZO-1, Occludin, Claudin), (sIgA) and SCFAs as well as decreased expression of lipopolysaccharides (LPS) in colonic tissues. To explore the role of QLT capsule in regulating

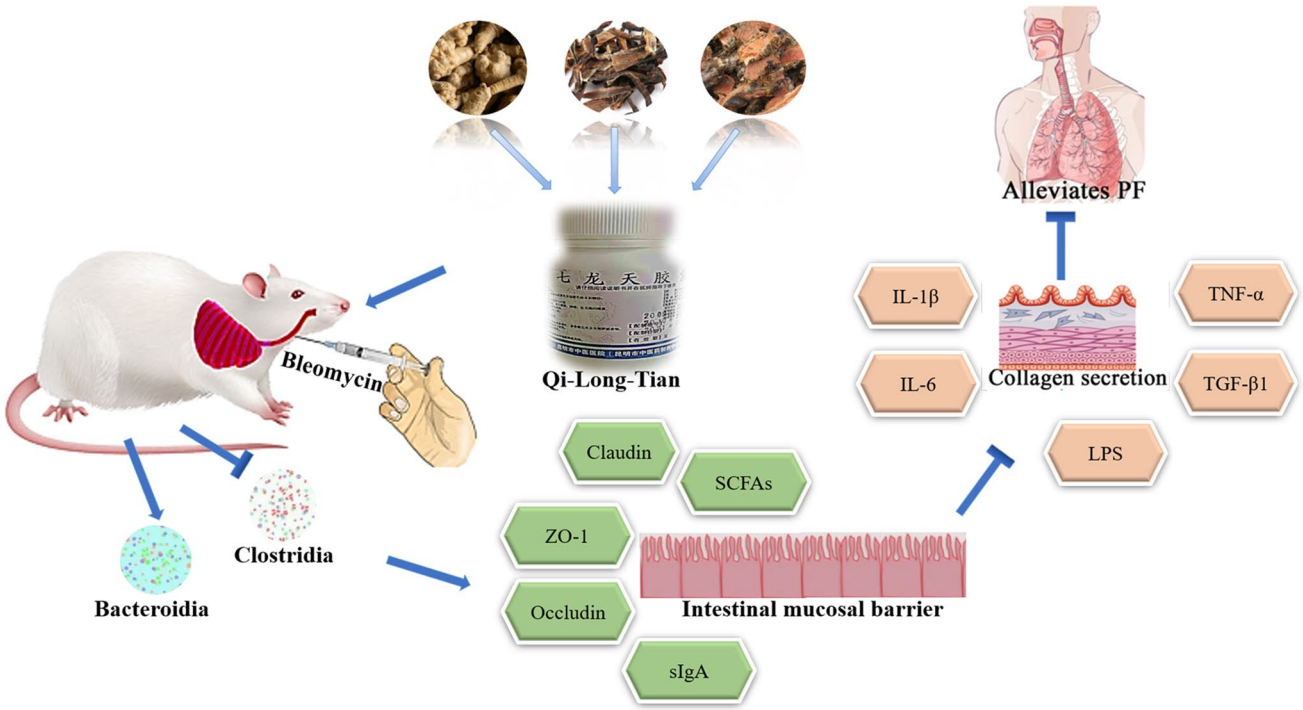

Fig. 11 The overall study concept of the article

enterobacterial microbes, we used 16S rRNA sequencing to analyze the abundance and differences in the composition of enterobacteria. The results indicated that QLT capsule alters the composition of GM. Further studies suggested that the changes of *Bacteroidia* and *Clostridia* in GM were associated with the inflammatory metabolic pathways and pro-inflammatory factor-related indicators for the development of PF. The above results clarified the therapeutic mechanism of QLT capsule to regulate intestinal flora, reduce the inflammatory response, and intervene in PF, which provides a theoretical basis for its further clinical application.

Supplementary Information The online version contains supplementary material available at https://doi.org/10.1007/s10142-023-00988-3.

Acknowledgements This research was funded by the research on the comprehensive efficacy evaluation of "Tian Long Dao" stage-based treatment program on IPF (The key project of Yunnan Provincial Science and Technology of Chinese Medicine Association) [No. 2017FF117(-007)]. This research was supported by Yunnan Provincial Key Laboratory of Molecular Biology for Sinomedicine, China (No. 2019DG016).

Author contribution Q. Z. and T. L. did the conception and designed of the study. D. -Z. Y. and J. L. drafted the article and revised it critically for important intellectual content. Y. F. and J. -L. Y. approved of the version to be submitted. All authors have read and agreed to the published version of the manuscript.

Data availability The raw data supporting the conclusions of this manuscript will be made available by the authors, without undue reservation, to any qualified researcher.

Declarations

Ethics approval and consent to participate The animal study protocol was approved by the Animal Care and Welfare Committee of Yunnan University of Chinese Medicine (protocol code: R-06202023, June 15th, 2020).

Conflict of interest The authors declare no competing interests.

References

Abdool Karim SS, Baxter C, Passmore JS et al (2019) The genital tract and rectal microbiomes: their role in HIV susceptibility and prevention in women. J Int AIDS Soc 22(5):e25300. https://doi.org/10.1002/jia2.25300

Adan RAH, van der Beek EM, Buitelaar JK et al (2019) Nutritional psychiatry: towards improving mental health by what you eat. Eur Neuropsychopharmacol 29(12):1321–1332. https://doi.org/10.1016/j.euroneuro.2019.10.011

Chen C, Xu P (2022) Activation and pharmacological regulation of inflammasomes. Biomolecules 12(7):1005–1010. https://doi.org/10.3390/biom12071005

Chen D (2018) Preliminary study on the mechanism of lung fibrosis in mice by Yilong dispersing knot formula. (Doctoral dissertation, Yunnan College of Traditional Chinese Medicine 2018: 1–15. http://cdmd.cnki.com.cn/Article/CDMD-10680-1018090629.htm. Accessed 9 Jun 2018

Chen CY (2011) TCM Database@Taiwan: the world's largest traditional Chinese medicine database for drug screening in silico. PloS one 6(1):e15939. https://doi.org/10.1371/journal.pone.0015939

Chopra N, Halkur SS, Biswas S et al (2021) Pulmonary tuberculosis presenting as acute respiratory distress syndrome. BMJ Case Rep 14(1):e237664. https://doi.org/10.1136/bcr-2020-237664

Choudhury S, Mansi MSK et al (2021) Genome-wide identification of Ran GTPase family genes from wheat (T. aestivum) and their expression profile during developmental stages and abiotic stress conditions. Funct Integr Genomics 21(2):239–250. https://doi.org/10.1007/s10142-021-00773-0

Chunxi L, Haiyue L, Yanxia L et al (2020) The gut microbiota and respiratory diseases: new evidence. J Immunol Res 2020:2340670. https://doi.org/10.1155/2020/2340670

Dai X, Mao C, Lan X et al (2017) Acute Penicillium marneffei infection stimulates host M1/M2a macrophages polarization in BALB/C mice. BMC Microbiol 17(1):177–186. https://doi.org/10.1186/s12866-017-1086-3

Ding Q, Zhu W, Diao Y et al (2021) Elucidation of the mechanism of action of ginseng against acute lung injury/acute respiratory distress syndrome by a network pharmacology-based strategy. Front Pharmacol 11:611794. https://doi.org/10.3389/fphar.2020.611794

Fu X, Yang C, Chen B et al (2021) Qi-Long-Tian formula extract alleviates symptoms of acute high-altitude diseases via suppressing the inflammation responses in rat. Respir Res 22(1):52. https://doi.org/10.1186/s12931-021-01645-8

Furman O, Tsoory M, Chen A (2022) Differential chronic social stress models in male and female mice. Eur J Neurosci 55(9–10):2777–2793. https://doi.org/10.1111/ejn.15481

Gong GC, Song SR, Su J (2021) Pulmonary fibrosis alters gut microbiota and associated metabolites in mice: an integrated 16S and metabolomics analysis. Life Sci 264:118616. https://doi.org/10.1016/j.lfs.2020.118616

Guan Z, Goldfine H (2021) Lipid diversity in clostridia. Biochim Biophys Acta Mol Cell Biol Lipids 1866(9):158966. https://doi.org/10.1016/j.bbalip.2021.158966

Gu GG, Teng H (2008) Shennong Bencao Jing. Hunan Sci Technol Press 03:1–69

Guo CJ (2021) Immune activation kickstarts the gut microbiota. Cell Host Microbe 29(3):318–320. https://doi.org/10.1016/j.chom.2021.02.012

Guzy RD, Li L, Smith C et al (2017) Pulmonary fibrosis requires cell-autonomous mesenchymal fibroblast growth factor (FGF) signaling. J Biol Chem 292(25):10364–10378. https://doi.org/10.1074/jbc.M117.791764

Hsu YL, Hung JY, Chang WA et al (2017) Hypoxic lung cancer-secreted exosomal miR-23a increased angiogenesis and vascular permeability by targeting prolyl hydroxylase and tight junction protein ZO-1. Oncogene 36(34):4929–4942. https://doi.org/10.1038/onc.2017.105

Huang G, Khan I, Li X et al (2017) Ginsenosides Rb3 and Rd reduce polyps formation while reinstate the dysbiotic gut microbiota and the intestinal microenvironment in ApcMin/+ mice. Sci Rep 7(1):12552. https://doi.org/10.1038/s41598-017-12644-5

Huang JH, Huang XH, Chen ZY et al (2004) Dose conversion among different animals and healthy volunteers in pharmacological study. Chin J Clin Pharmacol Ther 9: 1069–1072. http://kns.cnki.net.https.gzlib.proxy.chaoxing.com/KCMS/detail/detail.aspx?dbname=cjfd2004&filename=ylzl200409025&dbcode=cjfq. Accessed 26 Oct 2004

Iacob S, Iacob DG (2019) Infectious threats, the intestinal barrier, and its trojan horse: dysbiosis. Front Microbiol 10:1676. https://doi.org/10.3389/fmicb.2019.01676

Ishaque S, Shamseer L, Bukutu C, Vohra S (2012) Rhodiola rosea for physical and mental fatigue: a systematic review. BMC Complement Altern Med 12:70. https://doi.org/10.1186/1472-6882-12-70

Jia W, Martin TA, Zhang G, Jiang WG (2013) Junctional adhesion molecules in cerebral endothelial tight junction and brain metastasis. Anticancer Res 33(6): 2353–2359. https://ar.iiarjournals.org/content/33/6/2353.long. Accessed 15 May 2013

Jia XF, Guo XB (2012) Improved rapid tracheal instillation in mice - study on oral direct vision instillation under transmission lamp. J Environ Health 29: 217–219. https://doi.org/10.16241/j.cnki.1001-5914.2012.03.022

Jówko E, Sadowski J, Długołęcka B et al (2018) Effects of Rhodiola rosea supplementation on mental performance, physical capacity, and oxidative stress biomarkers in healthy men. J Sport Health Sci 7(4):473–480. https://doi.org/10.1016/j.jshs.2016.05.005

Khan J, Noboru N, Young A, Thomas D (2017) Pro and anti-inflammatory cytokine levels (TNF-α, IL-1β, IL-6 and IL-10) in rat model of neuroma. Pathophysiology 24(3):155–159. https://doi.org/10.1016/j.pathophys.2017.04.001

Khan J, Sharma PK, Mukhopadhaya A (2015) Vibrio cholerae porin OmpU mediates M1-polarization of macrophages/monocytes via TLR1/TLR2 activation. Immunobiology 220(11):1199–1209. https://doi.org/10.1016/j.imbio.2015.06.009

Laferriere CA, Pang DS (2020) Review of intraperitoneal injection of sodium pentobarbital as a method of euthanasia in laboratory rodents. J Am Assoc Lab Anim Sci 59:254–263. https://doi.org/10.30802/AALAS-JAALAS-19-000081

Leng P, Yu XL, Wei DX et al (2016) Effect of Qilongtian on IL-1β and TNF-α in rats with influence of hypoxic pulmonary hypertension. J Beijing Univ Tradit Chin Med 39(11): 915–919. http://kns.cnki.net.https.gzlib.proxy.chaoxing.com/KCMS/detail/detail.aspx?dbname=cjfd2016&filename=jzyb201611006&dbcode=cjfq. Accessed 30 Nov 2016

Li L, Huang G, Chen T et al (2022) Fufang Fanshiliu decoction revealed the antidiabetic effect through modulating inflammatory response and gut microbiota composition. Evid Based Complement Alternat Med 2022:3255401. https://doi.org/10.1155/2022/3255401

Li N, Liu TH, Liu Y, et al. (2019) Curcumin and curcumol inhibit NF-κB and TGF-β1 /Smads signaling pathways in CSE-Treated RAW246.7 Cells. Evidence-based complementary and alternative medicine 2019:3035125. https://doi.org/10.1155/2019/3035125

Limeta A, Ji B, Levin M et al (2020) Meta-analysis of the gut microbiota in predicting response to cancer immunotherapy in metastatic melanoma. JCI Insight 5(23):e140940. https://doi.org/10.1172/jci.insight.140940

Ling Z, Jin C, Xie T et al (2016) Alterations in the fecal microbiota of patients with HIV-1 infection: an observational study in a Chinese population. Sci Rep 6:30673. https://doi.org/10.1038/srep30673

Liu XJ, Yao HY, Tu Y et al (2018) Effect of respiratory rehabilitation training combined with Kerun capsule on inflammatory response and pulmonary fibrosis in patients with silicosis complicated by COPD. J Hainan Med Coll 24(04):480–483. https://doi.org/10.13210/j.cnki.jhmu.20180203.006

Liu Y, Zhang Y, Li S, Cui J (2021) Gene expression pattern of trophoblast-specific transcription factors in trophectoderm by analysis of single-cell RNA-seq data of human blastocyst. Funct Integr Genomics 21(2):205–214. https://doi.org/10.1007/s10142-021-00770-3

Lv D, Yang HN, Liu CHC et al (2021) Responses and key gene expression of inflammatory and oxidative stress factors associated with lung fibrosis in silica-dyed mice. J Environ Occup 38(10):1150–1155. https://doi.org/10.13213/j.cnki.jeom.2021.21061

Martin TA, Jiang WG (2009) Loss of tight junction barrier function and its role in cancer metastasis. Biochim Biophys Acta 1788(4):872–891. https://doi.org/10.1016/j.bbamem.2008.11.005

Mercader-Barceló J, Truyols-Vives J, Río C et al (2020) Insights into the role of bioactive food ingredients and the microbiome in idiopathic pulmonary fibrosis. Int J Mol Sci 21(17):6051. https://doi.org/10.3390/ijms21176051

Meyer NJ, Gattinoni L, Calfee CS (2021) Acute respiratory distress syndrome. Lancet 398(10300):622–637. https://doi.org/10.1016/S0140-6736(21)00439-6

Milton PL, Dickinson H, Jenkin G et al (2012) Assessment of respiratory physiology of C57BL/6 mice following bleomycin

administration using barometric plethysmography. Respiration 83:253–266. https://doi.org/10.1159/000330586
Nakerakanti S, Trojanowska M (2012) The role of TGF-β1 receptors in fibrosis. Open Rheumatol J 6:156–162. https://doi.org/10.2174/1874312901206010156
Nie H, Zheng M, Wang Z et al (2021) Transcriptomic analysis provides insights into candidate genes and molecular pathways involved in growth of Manila clam Ruditapes philippinarum. Funct Integr Genomics 21(3–4):341–353. https://doi.org/10.1007/s10142-021-00780-1
Panossian A, Wikman G, Sarris J (2010) Rosenroot (Rhodiola rosea): traditional use, chemical composition, pharmacology and clinical efficacy. Phytomedicine 17(7):481–493. https://doi.org/10.1016/j.phymed.2010.02.002
Paquin-Proulx D, Ching C, Vujkovic-Cvijin I et al (2017) Bacteroides are associated with GALT iNKT cell function and reduction of microbial translocation in HIV-1 infection. Mucosal Immunol 10(1):69–78. https://doi.org/10.1038/mi.2016.34
Pi AN (2020) Effects of Yunyao "Qilongtian" on pulmonary function and TGF-β1, MMP9 serum level in stable COPD patients. Yunnan Univ Tradit Chin Med 2020:1–9. http://kns.cnki.net.https.gzlib.proxy.chaoxing.com/KCMS/detail/detail.aspx?filename=1020086510.nh&dbname=CMFDTEMP. Accessed 1 May 2020
Pu WL, Zhang MY, Bai RY et al (2020) Anti-inflammatory effects of Rhodiola rosea L.: a review. Biomed Pharmacother 121:109552. https://doi.org/10.1016/j.biopha.2019.109552
Roberts AP, Hughes AW (1985) Complications with antibiotics used prophylactically in joint replacement surgery: a case report of cephradine-induced pseudomembranous colitis. Int Orthop 8(4):299–302. https://doi.org/10.1007/BF002668
Ru J, Li P, Wang J et al (2014) TCMSP: a database of systems pharmacology for drug discovery from herbal medicines. J Cheminform 6:13
Sato K, Yoshida K, Takumi S (2021) RNA-Seq-based DNA marker analysis of the genetics and molecular evolution of Triticeae species. Funct Integr Genomics 21(5–6):535–542. https://doi.org/10.1007/s10142-021-00799-4
Schneiderhan J, Master-Hunter T, Locke A (2016) Targeting gut flora to treat and prevent disease. J Fam Pract 65(1):34–38
Schönherr-Hellec S, Aires J (2019) Clostridia and necrotizing enterocolitis in preterm neonates. Anaerobe 58:6–12. https://doi.org/10.1016/j.anaerobe.2019.04.005
Shaw TD, McAuley DF, O'Kane CM (2019) Emerging drugs for treating the acute respiratory distress syndrome. Expert Opin Emerg Drugs 24(1):29–41. https://doi.org/10.1080/14728214.2019.1591369
Shizhen Li (2019) The compendium of materia medica. Line Book Bureau 01:150–171
Stecher B (2015) The roles of inflammation, nutrient availability and the commensal microbiota in enteric pathogen infection. Microbiol Spectr 3(3):297–320. https://doi.org/10.1128/microbiolspec.MBP-0008-2014
Totsch SK, Meir RY, Quinn TL et al (2018) Effects of a standard American diet and an anti-inflammatory diet in male and female mice. Eur J Pain 22(7):1203–1213. https://doi.org/10.1002/ejp.1207
Tucker LB, Burke JF, Fu AH, McCabe JT (2017) Neuropsychiatric symptom modeling in male and female C57BL/6J mice after experimental traumatic brain injury. J Neurotrauma 34(4):890–905. https://doi.org/10.1089/neu.2016.4508
Venturin GL, Chiku VM, Silva KL et al (2016) M1 polarization and the effect of PGE2 on TNF-α production by lymph node cells from dogs with visceral leishmaniasis. Parasite Immunol 38(11):698–704. https://doi.org/10.1111/pim.12353
Walker TB, Robergs RA (2006) Does Rhodiola rosea possess ergogenic properties? Int J Sport Nutr Exerc Metab 16(3):305–315. https://doi.org/10.1123/ijsnem.16.3.305
Wu N, Sun H, Zhao X et al (2021) MAP3K2-regulated intestinal stromal cells define a distinct stem cell niche. Nature 592(7855):606–610. https://doi.org/10.1038/s41586-021-03283-y
Wu Y, Wang T, Qiao L, Lin H (2022) Upregulated microRNA-210-3p improves sevoflurane-induced protective effect on ventricular remodeling in rats with myocardial infarction by inhibiting ADCY9. Funct Integr Genomics 22(3):279–289. https://doi.org/10.1007/s10142-021-00816-6
Wu Y, Zhang F, Yang K et al (2019) SymMap: an integrative database of traditional Chinese medicine enhanced by symptom mapping. Nucleic Acids Res 47(D1):D1110–D1117
Xia W, Khan I, Li XA et al (2020a) Adaptogenic flower buds exert cancer preventive effects by enhancing the SCFA-producers, strengthening the epithelial tight junction complex and immune responses. Pharmacol Res 159:104809. https://doi.org/10.1016/j.phrs.2020.104809
Xia W, Li X, Su L et al (2020b) Corrigendum to "lycium berry polysaccharides strengthen gut microenvironment and modulate gut microbiota of the mice." Evid Based Complement Alternat Med 2020:4840656. https://doi.org/10.1155/2020/4840656
Yao Y, Cai X, Fei W et al (2022) The role of short-chain fatty acids in immunity, inflammation and metabolism. Crit Rev Food Sci Nutr 62(1):1–12. https://doi.org/10.1080/10408398.2020.1854675
Yu XL, Zhang XM, Zhang YX (2021) Study on action mechanism of Buqi Huoxue Tongluo formula on idiopathic pulmonary fibrosis based on bioinformations. Glob Tradit Chin Med 14(02): 209–214. http://kns.cnki.net.https.gzlib.proxy.chaoxing.com/KCMS/detail/detail.aspx?dbname=cjfd2021&filename=hqzy202102007&dbcode=cjfq. Accessed 6 Feb 2021
Zhan X, Liu B, Tong ZH (2020) Current status and considerations of pulmonary fibrosis after novel coronavirus pneumonia inflammation. Chin J Tuberc Respir 43(09):728–732. http://kns.cnki.net.https.gzlib.proxy.chaoxing.com/KCMS/detail/detail.aspx?dbname=cjfd2020&filename=zhjh202009018&dbcode=cjfq. Accessed Oct 2020
Zhang MZ, Yao B, Yang S et al (2012) CSF-1 signaling mediates recovery from acute kidney injury. J Clin Invest 122(12):4519–4532. https://doi.org/10.1172/JCI60363
Zhang Q, Luo T, Yuan DZ et al (2022) Study on the mechanism of action of Qilongtian in intervening pulmonary fibrosis in bleomycin model mice. J Shanghai Univ Tradit Chin Med 36(05):60–68. http://kns.cnki.net.https.gzlib.proxy.chaoxing.com/KCMS/detail/detail.aspx?dbname=cjfdtemp&filename=shzd202205011. Accessed 25 Oct 2022
Zhao CC, Wu XY, Yi H et al (2021a) The therapeutic effects and mechanisms of salidroside on cardiovascular and metabolic diseases: an updated review. Chem Biodivers 18(7):e2100033. https://doi.org/10.1002/cbdv.202100033
Zhao L, Cho WC, Nicolls MR (2021b) Colorectal cancer-associated microbiome patterns and signatures. Front Genet 12:787176. https://doi.org/10.3389/fgene.2021.787176

Zhao XY, Li B, Cao LY et al (2009) Opening of tight junction of human brain microvascular endothelial cells induced by small cell lung cancer cells. Adv Anat Sci 15(02):183-187,191. https://doi.org/10.16695/j.cnki.1006-2947.2009.02.027

Zhou CB, Zhou YL, Fang JY (2021) Gut microbiota in cancer immune response and immunotherapy. Trends Cancer 7(7):647–660. https://doi.org/10.1016/j.trecan.2021.01.010

Authors and Affiliations

Qiang Zhang[1] · Ting Luo[2] · Dezheng Yuan[3] · Jing Liu[3] · Yi Fu[4] · Jiali Yuan[1]

[1] School of Basic Medicine, Shanghai University of Traditional Chinese Medicine, Shanghai 201203, China

[2] Yunnan Provincial Key Laboratory of Molecular Biology for Sinomedicine, Yunnan University of Chinese Medicine, Kunming 650500, China

[3] School of Clinical Medicine, Yunnan University of Chinese Medicine, Kunming 650500, China

[4] Department of Pulmonary Diseases, Kunming Hospital of Traditional Chinese Medicine, 650500 Kunming, China